

Bowlics: history, advances and applications

Ling Wang, Dali Huang, Lui Lam & Zhengdong Cheng

To cite this article: Ling Wang, Dali Huang, Lui Lam & Zhengdong Cheng (2017) Bowlics: history, advances and applications, Liquid Crystals Today, 26:4, 85-111, DOI: 10.1080/1358314X.2017.1398307

To link to this article: <https://doi.org/10.1080/1358314X.2017.1398307>



© 2017 The Author(s). Published by Informa UK Limited, trading as Taylor & Francis Group.



Published online: 01 Dec 2017.



Submit your article to this journal [↗](#)



View related articles [↗](#)



View Crossmark data [↗](#)

Bowlics: history, advances and applications

Ling Wang^a, Dali Huang^a, Lui Lam^b and Zhengdong Cheng^a

^aArtie McFerrin Department of Chemical Engineering, Texas A&M University, College Station, TX, USA; ^bDepartment of Physics and Astronomy, San Jose State University, San Jose, CA, USA

ABSTRACT

There are three types of liquid crystals (LCs) in the world: rodics, discotics and bowlics, corresponding to one-, two- and three-dimensional molecules, respectively. The rodics were discovered by the Austrian, F. Reinitzer, in 1888 and is the material behind the LC display industry of \$100 billion annually. The discotics were discovered by S. Chandrasekhar's team in India, in 1977. The third type, bowlics, was proposed by a Chinese, LIN Lei (Lui LAM), in 1982 while working at the Institute of Physics, CAS, Beijing. Distinguished from the rodic and the discotic, a bowlic molecule breaks the up-down symmetry, and bowlic LCs are one of excellent candidates for switchable ferroelectrics with great potential applications in ultrahigh-density memory devices. The importance of strategic bowlic materials has recently attracted increasing attention of scientists from multiple disciplines and engineers from different backgrounds. In this review, the history of bowlics and their recent advances in molecular design, synthesis and applications are discussed.

KEYWORDS

Bowlics; liquid crystals; polar columns; switchable ferroelectrics

1. Introduction

Liquid crystals (LCs) are known as the fourth state of matter after solid, liquid and gaseous states^[1]. Due to the unique combination of orientational order and fluidic properties, LCs are now playing an increasingly significant role in bio-science, materials science, nanoscience and nanotechnology. The research of LCs has highly evolved from just a scientific curiosity in the beginning to the truly interdisciplinary and cutting-edge sciences that combine basic aspects of physics, chemistry, engineering and biology [2–17]. LCs have become quintessential materials in our daily life since the first discovery of LC phase in rodic (rod-like) molecules by the collaboration of Austrian botanist F. Reinitzer and German physicist Otto Lehmann in the nineteenth century (Figure 1(a)) [18,19]. LC displays (LCDs) based on rodic LCs have become one of the most important foundations of modern advanced information technology, which dominate the global market of advanced information displays with an annual worth of more than \$100 billion and drastically revolutionised the way that information is presented [20–26]. In 1977, Indian chemist S. Chandrasekhar demonstrated that not only rodic molecules but also discotic (disc-like) molecules could form liquid-crystalline phases as predicated by theoretical simulation (Figure 1(b)) [27–29]. Discotic LCs have now been considered as a new promising generation of organic semiconductors as well as

mesophase semiconductors due to their remarkable electronic and optoelectronic device performances [30–32]. Interestingly, ferroelectricity was discovered in the symmetry-breaking liquid-crystalline systems including chiral rod-like molecules, chiral discotic molecules and non-chiral banana-shaped molecules, which led to a very intense research activity of polar LCs [33–35].

In 1982, Chinese physicist LIN Lei (Lui LAM) first proposed the concept of bowlic (bowl-like) LCs by considering the 'dimensionality' of molecules (Figure 1(c)) [36]. He pointed out that in bowlic mesophases, the steric effect of molecules makes the compensation of permanent dipoles difficult and then the $\mathbf{n} \rightarrow -\mathbf{n}$ symmetry (where \mathbf{n} is the director) valid in the rodic and the discotic may break down. Therefore, bowlic LCs may possess some special physical properties, such as genuine ferroelectricity, second-harmonic generation (SHG) etc. [37–40]. The experimental existence of bowlic monomers (Figure 2(a)) was soon reported in cyclotriveratrylene (CTV)-based bowlic molecules by European scientists in 1985 (also called pyramidic [41] or cone-shaped [42]), and X-ray structural study of these mesophases was carried out [43]. Furthermore, bowlic polymers were also predicted by Lin in 1988 [44] and synthesised by Er-Man Zeng, a Chinese PhD student while doing his PhD thesis at Georgia Institute of Technology, USA [45]. Distinguished from the rodic

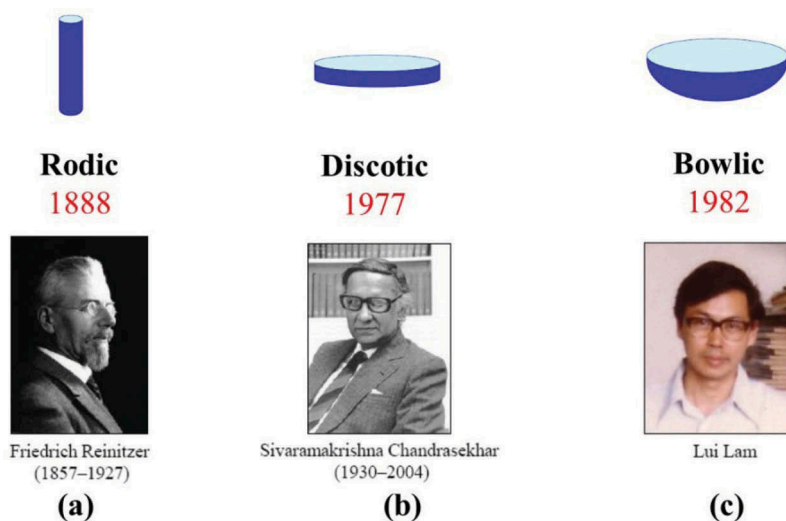


Figure 1. Three types of liquid crystals and their discoverers: (a) rodic (1D), (b) discotic (2D) and (c) bowlic (3D).

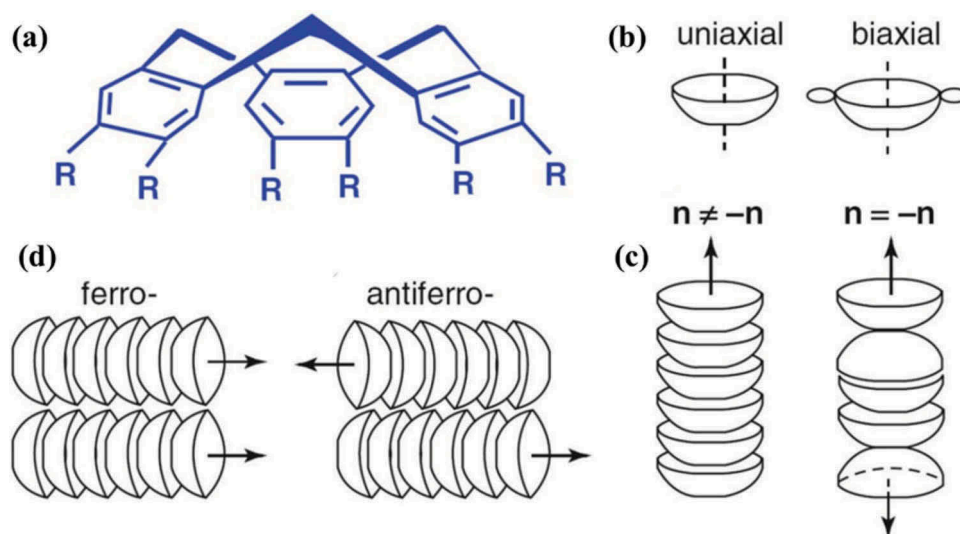


Figure 2. (a) Cyclotrimer-based bowl molecule, (b) uniaxial and biaxial bowls, (c) polar and non-polar columns made up of bowl molecules, (d) two types of column packing: ferroelectric (left) and antiferroelectric (right).

and discotic molecules, a bowl molecule is truly three dimensional (3D); bowl molecules are asymmetric in the up and down direction. Bowl molecules may have different symmetries as shown in Figure 2(b) and the corresponding phases could be either uniaxial or biaxial. The packing of bowls into columns may have specific features. For example, when all molecules in the column are oriented bottom down, then the head-to-tail symmetry is broken and the column has conical, i.e. polar symmetry $C_{\infty v}$ (Figure 2(c)). Only polar columns may form ferroelectric or antiferroelectric phases shown in Figure 2(d) [46]. In the bowl columns, the cones are embedded into one another with the same orientation, making the column axis polar. Such mesophases might therefore be ferroelectric, if all the columns adopted the

same polarisation direction within a macroscopic domain [47]. The unprecedented characteristics of bowl LCs could lead to new types of LCD with very fast response times and open a brand-new door for the development of ferroelectric or antiferroelectric soft materials with great potential applications in ultra-high-density memory devices and beyond. Since the discovery, a large number of bowl molecules with different LC phases have been designed and synthesised. In 1996 at the 16th International Liquid Crystal Conference in Kent, Ohio, the Glenn Brown Award for best PhD thesis was awarded to Bing Xu from Timothy Swager's group at University of Pennsylvania, for his work on bowl LCs [48]. Recently, switchable ferroelectric columns have been demonstrated in bowl LCs

[49], and liquid-crystalline behaviours of colloidal bowl-shaped nanoparticles have been investigated [50]. The term bowl or bowl LC is now recognised officially by the IUPAC [51] and formally in *Handbook of Liquid Crystals* [52].

In this review, we will start with the CTVs-based bowl LCs, where the effects of functional moieties such as flexible chains, mesogenic groups and dendritic molecules on the liquid-crystalline behaviours are discussed. We then introduce the design, synthesis and properties of calixarene-based bowl LCs with calamitic and discotic substitutions. We also address the new advances in bowl LCs including supramolecular bowl LCs, corannulene LCs, subphthalocyanine LCs, liquid-crystalline peptidic macrocycles and colloidal bowl-shaped nanoparticles. The last section of this review provides a perspective for the future scope of these emerging areas of bowl LCs. It should be noted that this work will not include all accomplishments in this research field but rather points to important developments by selecting representative examples from different research topics. We hope that this review will arouse increasing attentions of more researchers to such promising topics and future efforts would not only broaden our knowledge of soft matter but also promote their diverse applications as intelligent advanced functional materials.

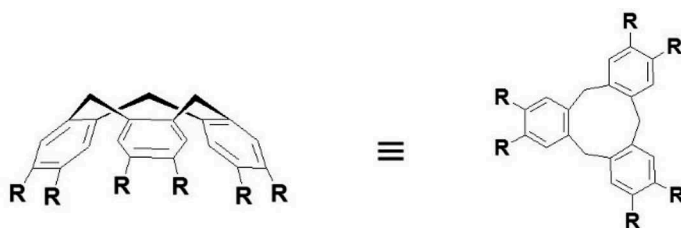
2. CTV-based LCs

2.1. CTVs with flexible chains

CTVs were first synthesised by Gertrude Robinson in 1915 but misdiagnosed as the dimer [53]. In 1965, Lindsey identified the correct structure and coined CTV as the name for the compound [54]. CTVs could exhibit either a crown conformation or a saddle conformation [55]. Its crown conformation provides a bowl-shaped structure, giving the molecule C_3 symmetry [56,57]. In 1985, Zimmermann et al. [41] and Malthete et al. [42] first reported the liquid-crystalline behaviours of CTV-based bowl molecules. Zimmermann et al. designed and synthesised two series of mesogenic compounds consisting of a rigid CTV central core and six equal flexible side chains, and their mesomorphic properties were studied by calorimetry and optical microscopy [41]. Two series of compounds are I-hexaalkoxytribenzocyclononene (compounds **1–10** in Table 1) and II-hexaalkanoyloxytribenzocyclononene (compounds **11–18** in Table 1). In series I, thermodynamically stable mesophases began to appear when the number of carbon atoms in each side chain, n , is equal

to or larger than six ($n \geq 6$), while for series II, all the compounds were found to exhibit mesomorphism ($n = 8–15$). They called these mesophases pyramidal mesophases (P), which are in fact bowl LC mesophases. They claimed that the mesophases P_A and P_C were optically uniaxial, while P_B and P_D were biaxial. Enantiotropic pyramidal mesophases were further observed in another homologous series of hexasubstituted tribenzocyclononene derivatives **19–22** [58]. Interestingly, these mesophases were found to exhibit an uncommon feature in that their optical anisotropy changed sign as function of temperature within the mesophase region. They assumed that these phases had columnar structures similar to those occurring in the conventional columnar discotics, which were confirmed by X-ray characterisations [43,59,60].

Budig et al. investigated the influence of heteroatoms and branchings on the liquid-crystalline properties of CTV derivatives **23–36** by incorporating heteroatoms (O or S) in different positions in the lateral chains (Table 2) [61]. Owing to the high melting points of compounds **23** and **24**, no mesophase was detected for these short-chain derivatives. All other esters displayed columnar mesophases, and the mesophase stability of the 3-oxaalkanoates was found to increase in comparison to the corresponding alkanoates. For example, compound **29** exhibits a clearing temperature which is $\sim 30^\circ\text{C}$ higher than that of the corresponding n -alkanoate **17**. Compound **31** that incorporated a divalent sulphur atom displayed approximately the same clearing temperature as the corresponding carbon analogue. Compounds **31–34**, in which the ether oxygens are shifted to the fourth positions, were found to exhibit a lower mesophase stability than the corresponding nalkanoates and the compounds with oxygen atoms in the third positions of the lateral chains. The cyclotribenzylene derivatives **35** and **36**, with bromine atoms or cyano groups at the termini of the side chains, did not display any liquid-crystalline phase. Moreover, it is particularly remarkable that branches in the middle of the lateral chains not only widened the mesophase range but also stabilise the mesophases significantly. The clearing temperatures of the branched compounds **30** and **34** are significantly higher than those of the comparable non-branched compounds. The mesophases of these cyclotribenzylens were studied by polarising microscopy and X-ray diffraction (XRD) measurements. For example, Figure 3 shows the liquid-crystalline textures of compounds **25** and **29** and the corresponding XRD patterns. The pattern of **25** displays a large number of interferences in the small-angle region (Figure 3(c)), which could be evaluated only on the base of an oblique cell (i.e. oblique

Table 1. Phase transition temperatures (in °C) and (in brackets) enthalpies (in kJ/mol) of CTV-based bowlic compounds **1–22** first reported by Zimmermann et al. In the table, K stands for crystal and P for pyramidal mesophases, i.e. bowlic mesophases.

Compound No.	R	Transition temperature (T/ °C) and enthalpies (ΔH / kJmol ⁻¹)
1	C ₁ H ₃ O-	K ₁ 232 I
2	C ₄ H ₉ O-	K ₁ 135.6 (22.1) I
3	C ₆ H ₁₁ O-	K ₁ 68.4 (21.7) K ₂ 103.8 (16.0) I
4	C ₆ H ₁₃ O-	K ₁ 40.9 (15.7) P _A 92.2 (14.4) I
5	C ₇ H ₁₅ O-	K ₁ 25.0 (21.1) P _A 79.9 (9.3) I
6	C ₈ H ₁₇ O-	K ₁ 24.9 (24.8) P _A 71.5 (6.9) I
7	C ₉ H ₁₉ O-	K ₁ 18.7 (28.6) P _A 66.1 (6.9) I
8	C ₁₀ H ₂₁ O-	K ₁ 25.5 (40.4) P _A 63.2 (6.7) I
9	C ₁₁ H ₂₃ O-	K ₁ 34.8 (56.0) P _B 44.2 (7.2) P _A 62.0 (5.7) I
10	C ₁₂ H ₂₅ O-	K ₁ 48.3 (76.0) P _A 61.6 (6.2) I
11	C ₈ H ₁₇ C(O)O-	K ₁ 5.2 (16.1) P _D 153.1 (31.0) I
12	C ₉ H ₁₉ C(O)O-	K ₁ 23.9 (28.2) P _D 152.6 (30.2) I
13	C ₁₀ H ₂₁ C(O)O-	K ₁ 18.2 (22.1) K ₂ 32.7 (14.8) P _D 146.2 (29.2) I
14	C ₁₁ H ₂₃ C(O)O-	K ₁ 31.5 (22.0) P _E 38.6 (17.3) P _D 131.6 (3.7) P _C 140.8 (18.8) I
15	C ₁₂ H ₂₅ C(O)O-	K ₁ 58.1 (48.4) P _D 118.8 (3.1) P _C 140.6 (20.2) I
16	C ₁₃ H ₂₇ C(O)O-	K ₁ 67.4 (67.0) P _D 99.5 (2.3) P _C 139.2 (20.9) I
17	C ₁₄ H ₂₉ C(O)O-	K ₁ 73.4 (81.0) P _D 81.4 (1.4) P _C 136.2 (18.5) I
18	C ₁₅ H ₃₁ C(O)O-	K ₁ 80.5 (118.4) P _C 134.6 (19.1) I
19	C ₇ H ₁₅ C ₆ H ₄ C(O)O-	K 33.0 (8.4) P ₁ 57.3 (0.2-2) P ₂ 149.1 (9.6) I
20	C ₈ H ₁₇ C ₆ H ₄ C(O)O-	K 12.0 P ₁ 21.3 (8.2) P ₂ 156.5 (13.8) I
21	C ₁₀ H ₂₁ C ₆ H ₄ C(O)O-	K 43.0 (7.8) P ₂ 162.0 (15.9) I
22	C ₁₀ H ₂₁ OC ₆ H ₄ C(O)O-	K 50.6 (4.8) P ₁ 100.0 (16.0) P ₂ 190.2 (20.4) I

columnar phase D_{ob}). The pattern of compound **29** proves the existence of a hexagonal lattice (i.e. hexagonal columnar phase D_{hd}).

2.2. CTVs with mesogenic moieties

Lunkwitz et al. reported two homologous series of CTV-based bowlic LCs **37–55** in which six calamitic cyanobiphenyl or phenylthiadiazole rigid cores were introduced via flexible spacers of different length to the macrocyclic cyclo-tribenzylene unit (Table 3) [62]. In the series of 4-cyanobiphenyl derivatives **37–41**, the melting points and the clearing temperatures were found to decrease with increasing chain length. Owing to the high melting points of the compounds with short spacers, no mesophases could be detected for compounds **37** and **39**, and only

monotropic phases were found for **38**. The other cyanobiphenyl derivatives **40** and **41** with long chains exhibited enantiotropic liquid-crystalline properties. The smectic A (S_A) phase was observed in these bowlic LCs as confirmed by the textural observations and the XRD pattern. Compared these compounds with related monomeric 4-cyanobiphenyl LCs (e.g. C₆H₁₃O–C₆H₄–C₆H₄–CN: Cr 57°C N 75.5°C I), it was found that appending the cyanobiphenyl mesogens to the cyclo-tribenzylene unit led to a significant mesophase stabilisation and the nematic phase of the monomeric 4-cyanobiphenyl LCs was replaced by S_A phases in the CTV derivatives. In addition, S_A phases were found to be easily supercooled to –30°C without crystallisation. Replacing one of the rigid mesogens with a methyl group resulted in a mesophase destabilisation (**42–44**), and the melting points and the crystallisation tendency were

Table 2. Transition temperatures (in °C) and associated enthalpy values (in kJ/mol, in brackets) of CTV-based bowlic compounds **23–36**. In the table, K stands for crystal and D for columnar mesophase.

Compound No.	R	Transition temperature (T/ °C) and enthalpies ($\Delta H/ \text{kJmol}^{-1}$)
23	C ₄ H ₉ OCH ₂ C(O)O-	K 175 I
24	C ₅ H ₁₁ OCH ₂ C(O)O-	K 161-163 I
25	C ₆ H ₁₃ OCH ₂ C(O)O-	K 140 (11.7) D _{ob} 156 (13.9) I
26	C ₇ H ₁₅ OCH ₂ C(O)O-	K 130 (14.8) D _{hd} 154 (8.9) I
27	C ₈ H ₁₇ OCH ₂ C(O)O-	K 123 (14.5) D _{hd} 160(11.1) I
28	C ₁₀ H ₂₁ OCH ₂ C(O)O-	K 109(14.2) D _{hd} 165(13.3) I
29	C ₁₂ H ₂₅ OCH ₂ C(O)O-	K 93(11.1) D _{hd} 164(12.9) I
30	C ₅ H ₁₁ CH(CH ₃)OCH ₂ C(O)O-	K ? D _{rd} 188 I(32.1) I
31	C ₈ H ₁₇ SCH ₂ C(O)O-	K 59 (8.0) D _{hd} 138 (14.0) I
32	C ₅ H ₁₁ O(CH ₂) ₂ C(O)O-	K 63-65 I
33	C ₉ H ₁₉ O(CH ₂) ₂ C(O)O-	K 20 (6.7) D 79 (2.2) I
34	C ₅ H ₁₁ CH(CH ₃)O(CH ₂) ₂ C(O)O-	K -8 (1.4) D 105 (13.3) I
35	Br(CH ₂) ₁₀ C(O)O-	K 78 I
36	NC(CH ₂) ₁₀ C(O)O-	K 63 I

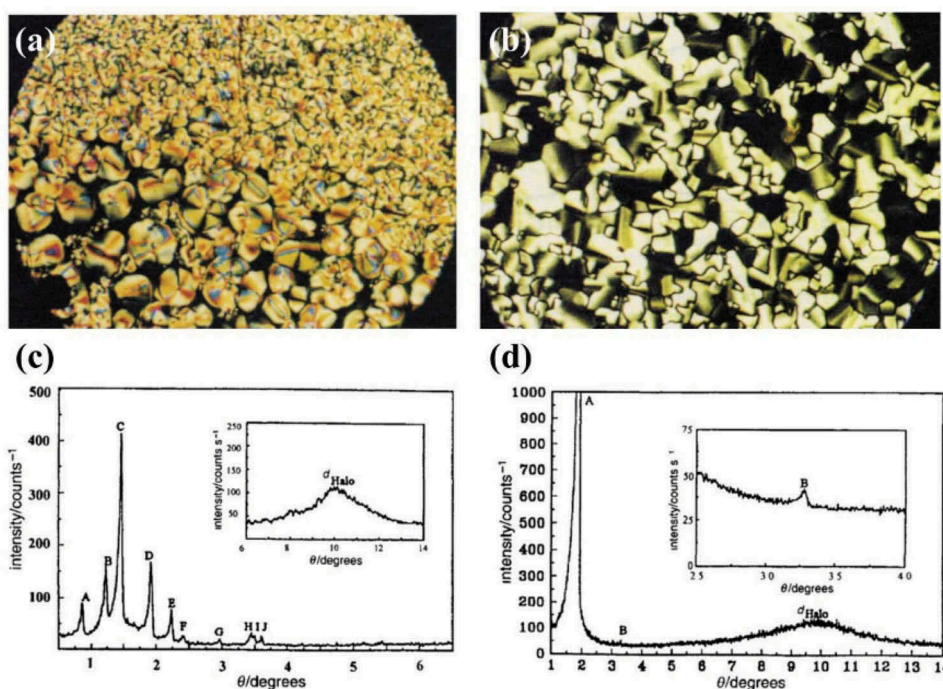
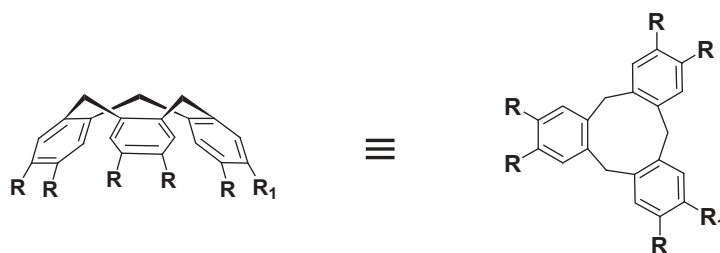


Figure 3. Optical photomicrographs under crossed polarisers of the mesophases of cyclotrimeratrylene derivatives as obtained by cooling from the isotropic melt: (a) D_{ob} phase of compound **25** at 155°C (b) D_{hd} phase of **29** at 138°C. The corresponding X-ray diffraction pattern of D_{ob} phase (c) and D_{hd} phase (d).

decreased by this desymmetrisation of the molecules. A monotropic S_A phase was observed by cooling the cyclotribenzylene derivative **42** which is a desymmetrised analogue of the non-liquid-crystalline compound **37**. In the series of the thiadiazole derivatives **45–55**, the phase behaviours were found to depend on the spacer length and

differ significantly from that of the above 4-cyanobiphenyl derivatives. The clearing temperatures decreased with the elongation of the spacer units, but the melting points of compounds kept nearly constant. The mesomorphic properties were only observed for the short chain derivatives and were lost on increasing the spacer length. The

Table 3. Transition temperatures (in °C) and associated enthalpy values (in kJ/mol, in brackets) of CTV-based bowlic LCs linked with six calamitic phenylthiadiazole or cyanobiphenyl rigid cores **37–55**. In the table, Cr stands for crystal, S_A for smectic A phase, S_x for unidentified smectic phase and Col for columnar mesophase.



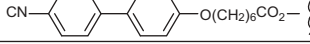
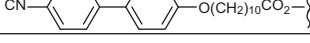
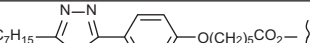
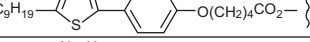
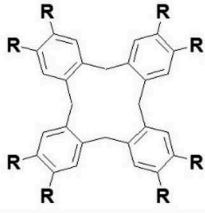
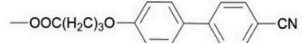
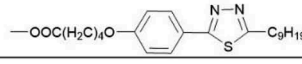
Compound No.	R ₁	R	Transition temperature (T/ °C) and enthalpies (ΔH/ kJmol ⁻¹)
37	R	CN-  -	Cr 220 (75.8) I
38	R	CN-  -	Cr 165 (76.6) [S _A 133 (6.6)] I
39	R	CN-  -	Cr 159 (83.9) I
40	R	CN-  -	Cr ₁ 65 (18.8) Cr ₂ 112 (7.0) S _A 123 (8.2) I
41	R	CN-  -	Cr ₁ 95 (58.3) S _A 116 (21.3) I
42	CH ₃	CN-  -	Cr 163 (40.4) [S _A 145] I
43	CH ₃	CN-  -	Cr 80 S _A 118 I
44	CH ₃	CN-  -	Cr 78 (48.3) S _A 107 (18.1) I
45	R	 -	Cr 152 (10.7) Col 182 (54.0) I
46	R	 -	Cr 117 S _A 159 I
47	R	 -	Cr 151 (30.6) Col 155 (65.8) I
48	R	 -	Cr 156 (144.9) I
49	R	 -	Cr 158 (135.6) I
50	R	 -	Cr 142 I
51	R	 -	Cr 152 S _A 160 I
52	R	 -	Cr ₁ 102 (87.1) Cr ₂ 143 (0.9) S _A 155 I
53	R	 -	Cr 80 Col 162 I
54	CH ₃	 -	Cr <20 S _x 126 S _A 142 I
55	CH ₃	 -	Cr 62 Col 148 I

Table 4. Transition temperatures (in °C) and associated enthalpy values (in kJ/mol, in brackets) of cyclotetraveratrylene (CTTV) derivatives **56–58**. In the table, Cr stands for crystal, N for nematic phase and M for mesophase.



Compound No.	R	Transition temperature (T/ °C) and enthalpies ($\Delta H/ \text{kJmol}^{-1}$)
56		Cr, 174(53.8) Cr, 222(63.6) N 220 I
57		Cr, 142(70.3) Cr, 204(10.6) M 222(44.5) I
58		Cr 241 I

compounds with an even number of methylene groups showed small focal conic fan textures, which can be homeotropically aligned on shearing the samples to give optically isotropic regions. These textural features are typical for S_A phases. The derivatives with an odd number of methylene groups were found to form highly viscous mesophases and display spherulitic flower textures which are typical of columnar mesophases (Col). Many other research also reported that depending on the length of the spacers connecting the central bowl-like CTV unit to the rod-like rigid cores, either columnar or smectic phases can be formed [63,64].

Lunkwitz et al. also investigated the liquid-crystalline properties in cyclotetraveratrylene (CTTV) derivatives **56–58** (Table 4), where CTTVs are much more flexible and sometimes are regarded as being disc-shaped molecules on the average [62]. In contrast to the CTV derivatives with S_A phases, the cyanobiphenyl derivative **56** is a nematic LC as is obvious from the typical nematic schlieren texture. A spherulitic texture was observed for the thiazole derivative **57** on cooling from the isotropic melt, which confirmed the absence of an S_A phase. The pyrimidine derivative **58** is a crystalline solid with no mesophase. Interestingly, in the case of the CTTV derivatives, columnar mesophases can be observed for compounds with an odd number of connecting atoms in the spacers. In the columnar phase, the CTTV core is believed to adopt the sofa form with C_{2h} symmetry [65,66].

2.3. CTVs with dendritic molecules

Collet et al. first reported the CTV-based mesogenic triester **59** which was functionalised with dendritic

molecules [67]. The hexagonal columnar phase was observed in both racemic and optically active forms (Figure 4). Percec and co-workers synthesised a series of dendritic CTVs and their self-organised supramolecular nanostructures were investigated by a combination of XRD methods and CD experiments [68,69]. The dendrimers **60–65** are representative examples (Figure 5), where the dendrimers include both hexa and tris substituted CTV cores with either chiral or achiral alkyl chains [69]. Interestingly, the dendritic CTVs could self-organise into bowl-like columns with a hexagonal lattice and/or into chiral supramolecular spheres (Figure 6). Different dendrimer types were found to exhibit different self-assembly behaviours. For example, only bowl-like

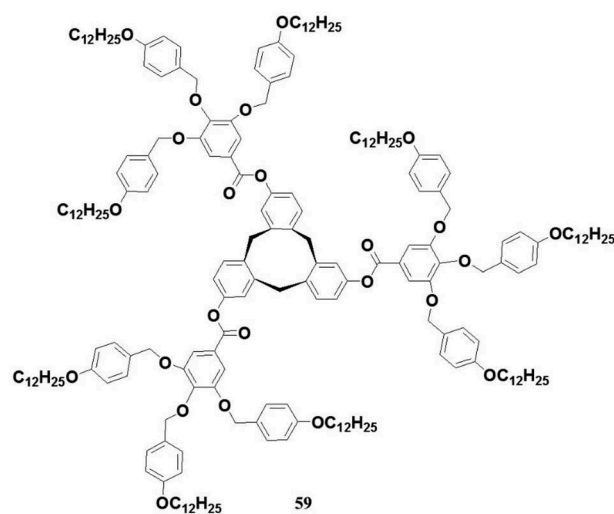


Figure 4. CTV-based mesogenic triester **59** which was functionalised with dendritic molecules.

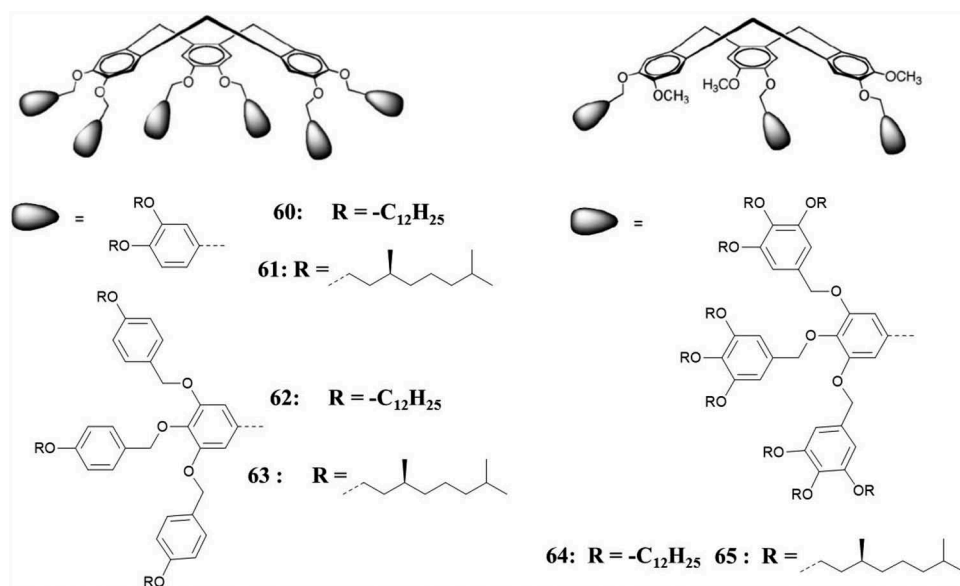


Figure 5. Chemical structures of dendronised cyclotrimeratrylene (CTV) derivatives **60–65**.

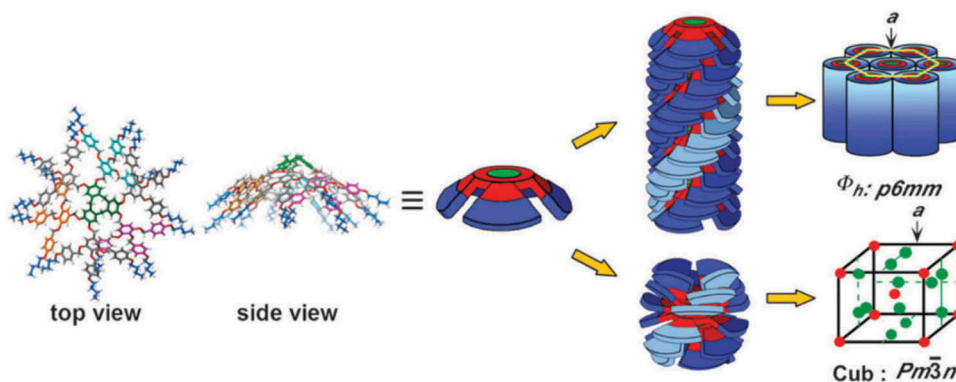


Figure 6. Schematic diagram of the self-assembly of dendritic CTVs into bowl-like columns or spheroidal assemblies. Columns self-organise into hexagonal lattice (top) while spheres organise into cubic (bottom) or tetragonal lattices.

columns were observed for both the achiral (**60**) and chiral (**61**) dendrimers, whereas dendrimers **64** and **65** were able to form only spherical assemblies. The dendrimers **62** and **63** showed different behaviour at different temperature according to whether the alkyl groups are chiral or achiral. The achiral **62** formed bowl-like columns at 100°C and chiral supramolecular spheres at 130°C , while its chiral analogue **63** formed only the supramolecular spheres. This new self-assembly process is expected to provide access to new mechanisms for the transfer and amplification of structural information from the molecular to supramolecular level and to generate new fundamental and technological concepts mediated by chiral supramolecular dendrimers.

3. Calixarene-based LCs

3.1. Calixarenes with calamitic moieties

Calixarenes are well-established building blocks as important as crown ethers and cyclodextrins in supramolecular chemistry [70–72]. They could be easily modified at the upper and lower rims with a large variety of functional groups and unique structures and work as novel receptors for binding all kinds of guests which may find potential applications in various fields such as ion and molecular recognition with fluorescent sensing, amino acid sensors, ion-selective electrode and chiral molecule recognition. A calix[4]arene with 4 units in the ring is known to exhibit a bowl-like conformation as shown in Figure 7 [73,74]. If LC groups are introduced onto the calixarene skeleton, the



Figure 7. (a) The structure of calix[4]arene, (b) schematic conformations and (c) 3D representation of a bowl-like conformation.

resulting derivatives are anticipated to show interesting bowl-like liquid-crystalline behaviours [75,76].

Cometti et al. first investigated the mesomorphic properties of bowl-like calix[4]arene core symmetrically surrounded by 12 flexible alkyl chains with variable length, and columnar mesophases were observed [77]. Tschierske et al. developed the exocalix[4]arenes **66–70** in which different calamitic rigid cores were linked to the macrocyclic calix[4]arene unit (Table 5) [78]. Upon incorporating the phenylthiadiazole units, these compounds were found to form a layered smectic A-type (S_A) mesophase. They claimed that in these derivatives of exocalix[4]arene, the calamitic rigid units determined the mesophase type. A columnar stacking of the molecules is not possible, but the calamitic units can adopt a parallel packing, which leads to the smectic self-organisation.

Yonetake et al. designed and synthesised calix[4]arene derivative **71**, and the liquid-crystalline properties were investigated [79]. As shown in Figure 8(b), a typical nematic schlieren texture with $s = \pm 1$ and $+1/2$

disclinations was observed at 76°C upon cooling. When the sample was further cooled, some stripes appeared immediately on the schlieren texture, and the stripe pattern became clear at room temperature (Figure 8(c)). Figure 8(d) shows the XRD pattern of **71** taken at room temperature. The sample was cooled from the isotropic and annealed at 70°C for 1 h. It exhibited two diffuse halos at the 2θ of approximately 5 and 20°. The d-spacings of the two halos at low and wide angles are about 1.5 and 0.43 nm, respectively. The halo at wide angle corresponds to the average distance between the neighbouring mesogens. The rings for the small angle area could be associated with the smectic layer structure. The layer spacing is estimated as 5.11 nm. Accordingly, the mesogen **71** exhibited nematic and smectic phases. The oriented XRD pattern under a magnetic field further revealed a smectic A phase with a layer spacing of 5.11 nm (Figure 8(e)).

Lo et al. reported a novel series of cone-conformed end-functionalised oligophenylene-substituted calix

Table 5. Transition temperatures (in °C) and associated enthalpy values (in kJ/mol, in brackets) of calix[4]arene derivatives **66–70**. In the table, Cr stands for crystal and S_A for smectic A phase.

Compound No.	R1	R2	R3	Transition temperature (T/ °C) and enthalpies (ΔH / kJmol ⁻¹)
66	CH ₃		H	Cr 159 (113) [S_A 149 (54)] I
67	CH ₃			Cr 196 (49) S_A 211 (29) I
68	C ₃ H ₇		H	Cr 126(126) I
69	C ₃ H ₇			Cr 150 S_A 165 I
70	CH ₃			Cr 168 (107) I

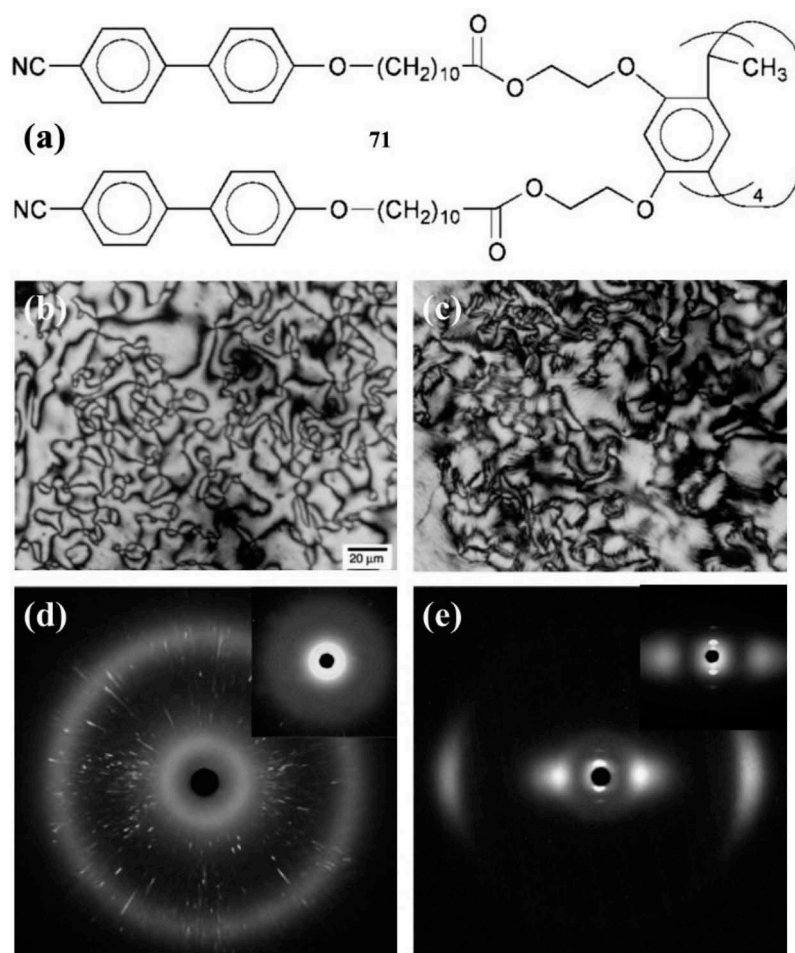


Figure 8. (a) Chemical structure of calix[4]arene derivative **71**; optical textures of **71** taken at (b) 76°C and (c) room temperature upon cooling using polarised optical microscope with crossed polarisers. XRD patterns of **71** (d) annealed at 70°C and (e) oriented in a magnetic field of 2.8 T.

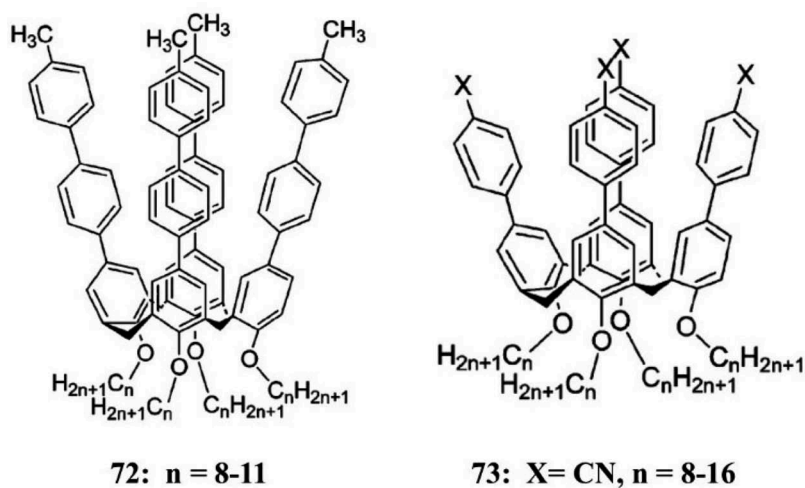


Figure 9. Chemical structures of end-functionalised oligophenylene-substituted calix[4]-arenes **72** and **73**.

[4]-arenes **72** and **73** (Figure 9) [80]. In contrast to the corresponding monomers, cyano-phenyl-calix[4]arene and methyl-biphenyl-calix[4]arene derivatives were found to exhibit highly ordered smectic supramolecular organisation as evidenced by the polarised optical microscopy and XRD studies. The optical textures of **73** were found to exhibit typical fanlike or mosaic texture, which suggest the ordered smectic mesophases (Figure 10(a–d)). Figure 10(e) shows the XRD measurements of **73** with $n = 9–16$, which further confirms the formation of the smectic layered structure. It was also found that the presence of the

strong dipoles in the rigid calixarene segments not only facilitates and stabilises the formation of the highly ordered smectic structure but also enhances the optical properties of calix[4]arene derivatives. These findings provide a new guideline to design interesting 3D bowl-like mesogenic materials.

Menon et al. reported the calix[4]arene Schiff bases **74–77** and their liquid-crystalline properties (Figure 11) [81]. All the compounds were found to exhibit nematic structure and a typical fanlike or mosaic texture, which suggests an ordered smectic mesophase. Dielectric investigations were also carried out and wide temperature range N, SmA and

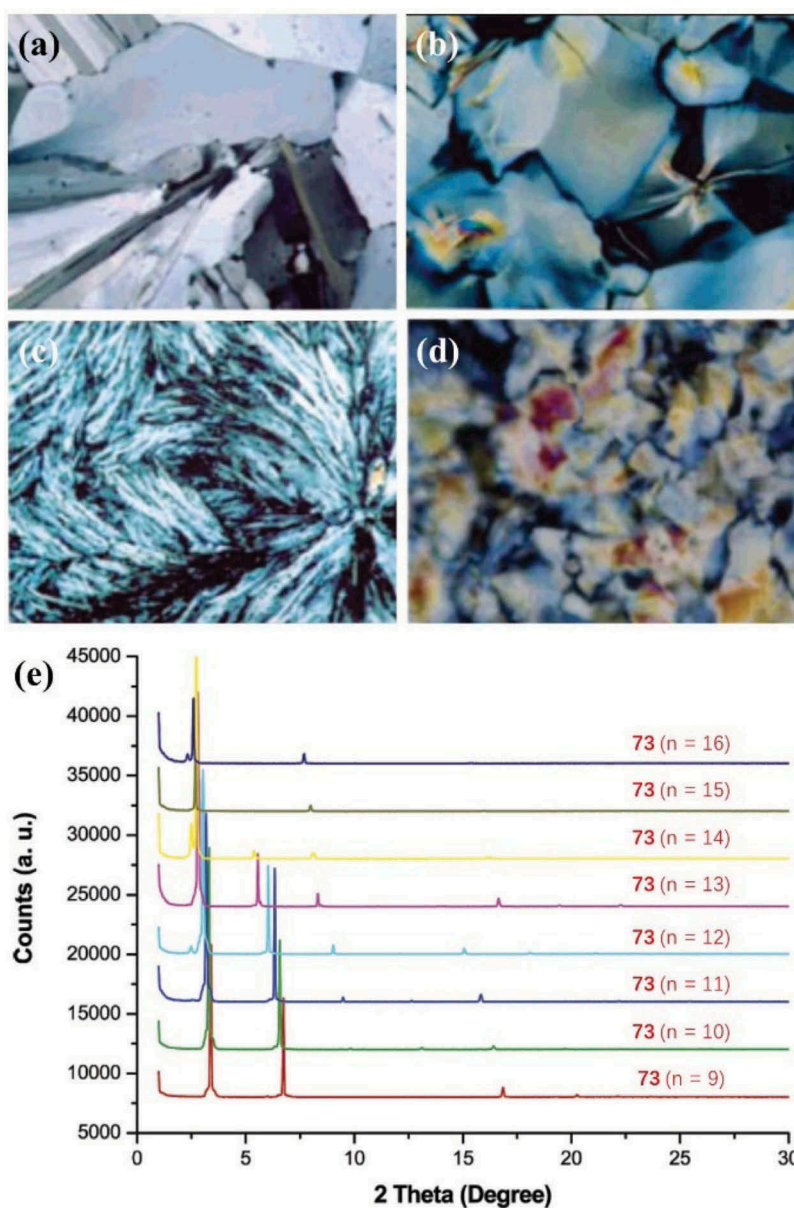
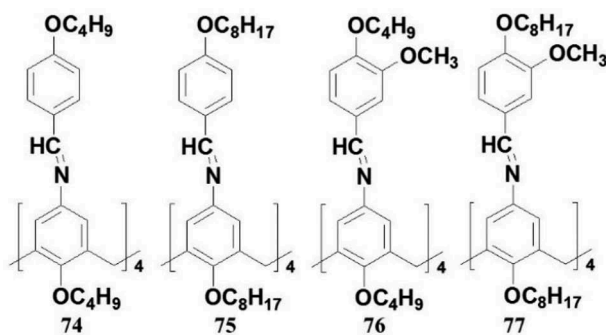


Figure 10. Some representative polarised optical microscope textures (200 \times) (a) **73** ($n = 11$) at 168°C, mosaic and lancet texture with some homeotropic area; (b) **73** ($n = 14$) at 148°C, mosaic texture; (c) **73** ($n = 15$) at 153°C, grass-like and fan-like texture; (d) **73** ($n = 9$) at 150°C, mosaic texture; (e) XRD patterns of frozen LC samples of **73** with $n = 9–16$ exhibiting multiple higher order reflections in the small angle area.



74: Cr 78.4 (42.3) SmC 99.2 (7.1) SmA 144.8 (8.3) N 180 (18.3) I

75: Cr 60.6 (34.1) SmC 91.2 (4.1) SmA 120.7 (6.2) N 173 (13.7) I

76: Cr 86.6 (55.0) SmC 99.1 (9.2) SmA 144.2 (2.3) N 185.1 (1.5) I

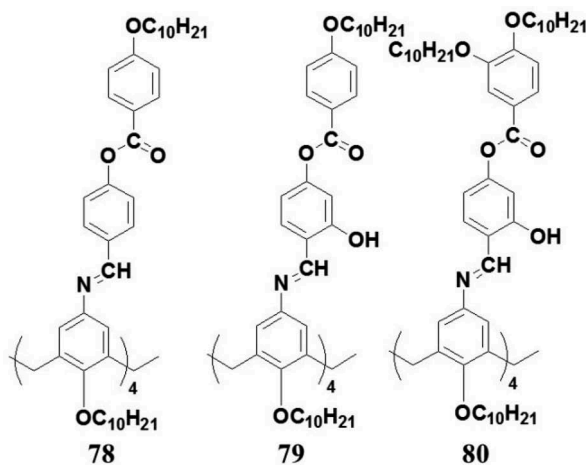
77: Cr 62.7 (40.2) SmC 118.8 (6.3) SmA 145 (8.8) N 175.9 (14.8) I

Figure 11. Chemical structures of calix[4]arene Schiff bases **74–77** and their liquid-crystalline properties. Cr: Crystal; SmA: smectic A mesophase; SmC: smectic C mesophase; N: nematic mesophase; I: isotropic liquid.

SmC phases were observed. These results indicated that the linking groups in the wide part have a large influence on the mesogenic properties of calixarene LCs [82]. Romero et al. synthesised liquid-crystalline calix[4]arene-appended Schiff bases **78–80** that exhibited a smectic A mesophase or a nematic phase depending on the number of terminal chains (Figure 12) [83]. Recently, Zhang et al. developed the calix[4]arene-cholesterol derivatives **81** with Schiff-base bridges (Figure 13(a)) [84]. They were found to exhibit the mesomorphic properties with the molecular arrangement of the calixarene bowl-like column and Schiff-based

cholesterol unit as ancillary lateral column. The mesophases disappeared upon the complexes of **81** with AgClO_4 (Figure 13(b)), which suggests that the mesophase of compounds **81** could be tuned by the ion-complexation behaviours.

Xu and Swage demonstrated the columnar LCs with a rigid bowl-like core based on oxo-tungsten calixarene complexes **82** and **83** (Figure 14(a)) [48]. The most dramatic consequence of host-guest complexation was its effect upon the mesomorphic behaviour of the complexes. While the $R = \text{H}$ analogue exhibited a



78: G 26 °C SmA 124 °C (3.6) I

79: G 26 °C SmA 57 °C (1.8) I

80: G 45 °C Cr 63 °C (-3.4) Cr' 105 °C N 114 °C (7.9) I

Figure 12. Chemical structures of calix[4]arene-appended Schiff bases **78–80** and their liquid-crystalline properties. G: Glass; Cr: crystal; SmA: smectic A mesophase; N: nematic mesophase; I: isotropic liquid.

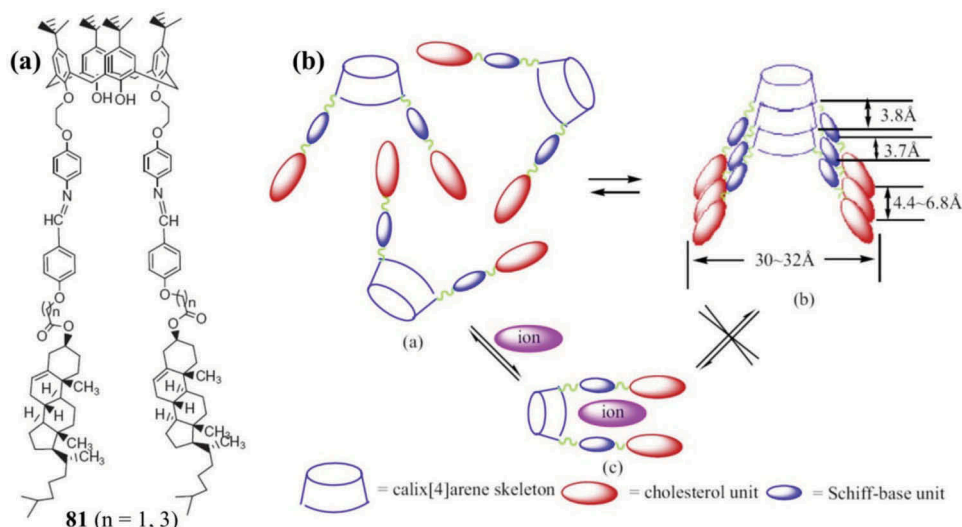


Figure 13. (a) Chemical structures of calix[4]arene–cholesterol derivatives. (b) Schematic representation of the columnar layered molecular arrangements and the complexation models.

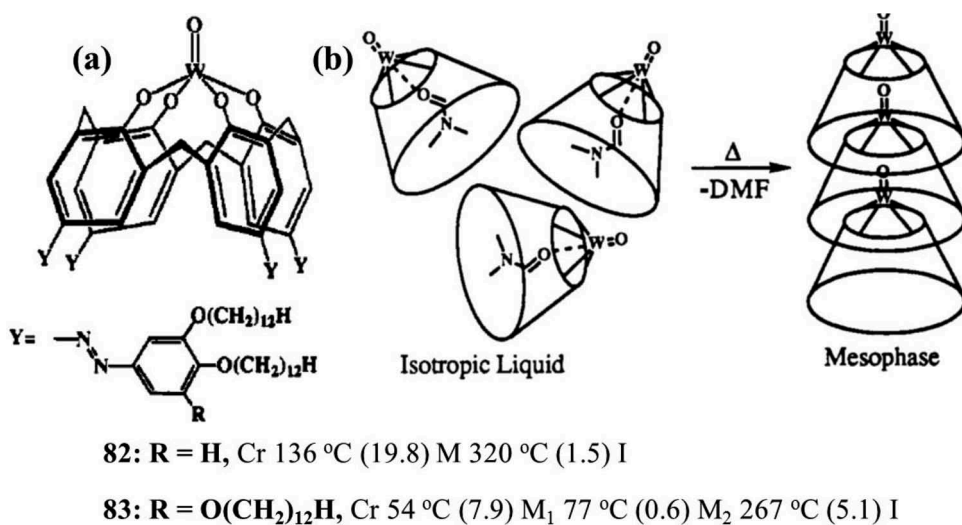


Figure 14. (a) The tungsten-oxo-based calixarenes and liquid-crystalline properties. (b) Illustration of how blocking of the cavity by the DMF guest prevents mesophase formation. Heating to temperatures greater than 200°C liberates DMF and allows the mesophase formation.

bowlic mesophase from 136 to 320°C, its DMF complex melted directly to an isotropic phase at 115°C. Likewise, the R = OC₁₂H₂₅ DMF complex melted to form an isotropic phase at 84°C. Complexes with pyridine guests were found to exhibit isotropic transitions at the same temperatures, indicating that a filled cavity is more important than the nature of the guest. With further heating (200–250°C), the DMF complex slowly dissociated to form the liquid-crystalline phase. The deleterious effect of a DMF or pyridine guest on the mesophase stability indicated that the occupation of cavity is critical to the formation of LCs (Figure 14(b)).

According to the columnar structure of the mesophases, it is assumed that the bowllic cores exhibited a head-to-tail arrangement whereby tungsten-oxo groups protrude into the cavity of the neighbouring mesogen.

Xu and Swager also investigated the host–guest mesomorphism of calixarene derivatives **84** (Figure 15) [85]. They demonstrated how host–guest principles could be used to stabilise a columnar bowllic phase of a conformationally flexible calix[4]arene. The uncomplexed conformationally flexible calix[4]arene **84a** was found to display a transient columnar

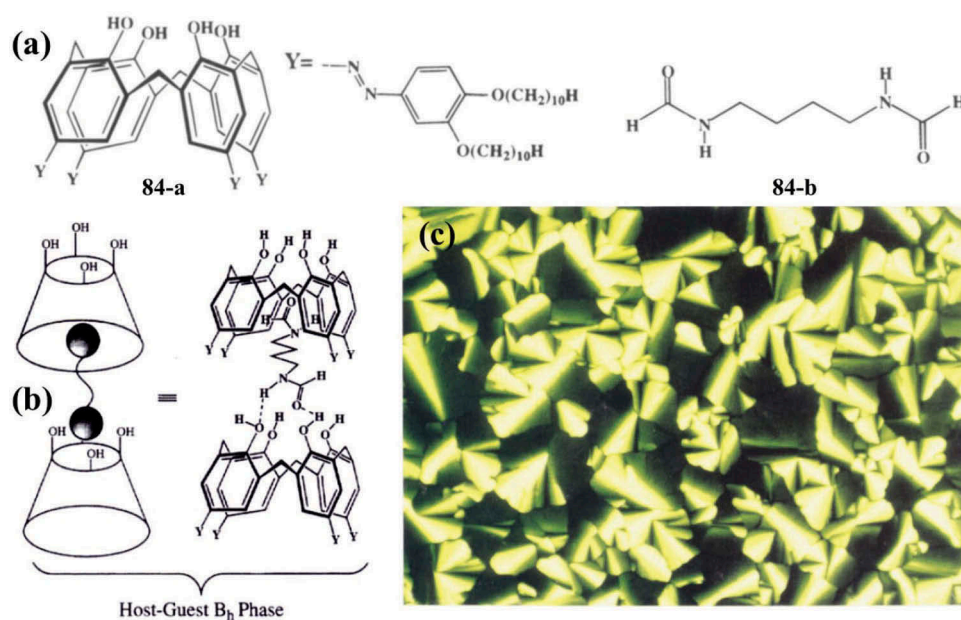


Figure 15. (a) Chemical structures of host-guest calixarene derivatives **84**. (b) Host-guest principles of stabilising a columnar bowllic (B_h) phase. (c) Optical texture of host-guest B_h phase (ratio of **84a**–**84b** is 2:1) taken with polarised optical microscope at 103°C.

bowlic mesophase which is only observed in the first heating. Further heating of **84a** to 163°C produces an isotropic phase, and subsequent cooling yields a non-birefringent solid material. They found that **84b** was especially effective for the formation of a host-guest mesophase with **84a**. The host-guest mesophase (ratio of **84a**–**84b** is 2:1) displayed high fluidity and thermodynamic stability over a 40°C range. They proposed that the function of **84b** is as shown in Figure 15(b), where one amide hinds in the cavity and enforces the cone conformation while the other forms hydrogen bonds with the nearest neighbour, thereby inducing head-to-tail organisations.

Sutariya et al. designed series of lower rim azocalix[4]arene bowllic mesogens **85** (Figure 16) with a flexible aliphatic chain and a rigid scaffold [86]. These

compounds were found to exhibit smectic C and nematic phases upon heating and cooling conditions. Interestingly, the introduction of azo groups enables them to respond upon external light irradiations. Moreover, novel gallic-calixarene derivatives with columnar phases were recently designed and synthesised (**86** and **87**) [87]. These mesomorphic studies suggested that the conformation plays a crucial role for bowllic calixarene LCs and the stable cone conformation is favourable for excellent mesomorphic property.

3.2. Calixarenes with discotic triphenylene moieties

Yang's group made several efforts to develop the bowllic calix[4]arene LCs by linking discotic triphenylene

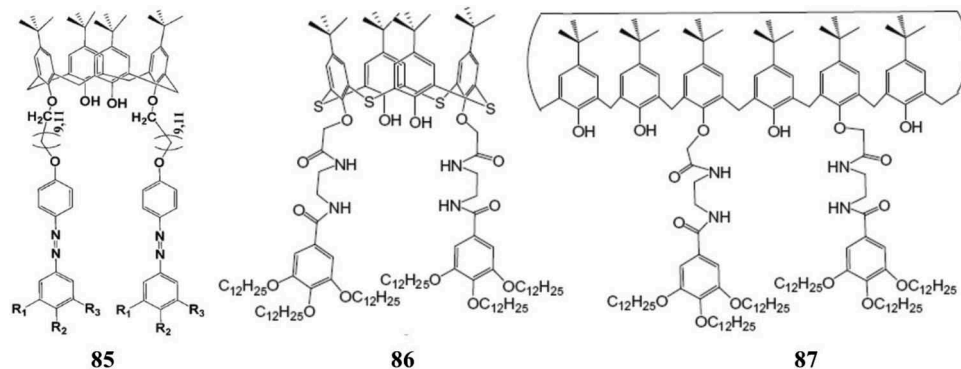


Figure 16. Chemical structures of azocalix[4]arene bowllic mesogens (**85**) and gallic-calixarene derivatives with columnar phases (**86** and **87**).

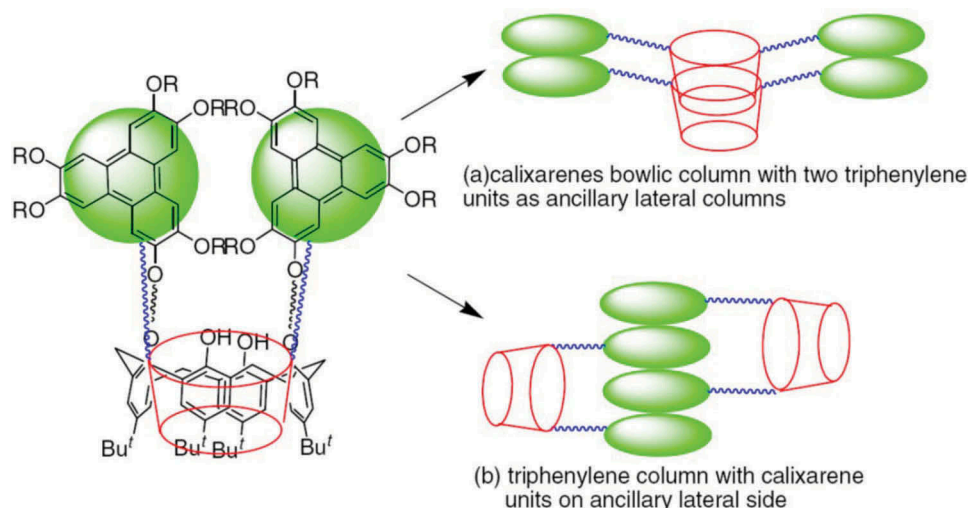


Figure 17. Two kinds of schematic representation of the columnar layered molecular arrangement for triads of triphenylene-calixarene-triphenylene.

[75]. In theory, there are two possible mesomorphic staking behaviours for LCs of calix[4]arene-linked triphenylene dimers as shown in Figure 17. One way is calixarene as cores, that is calixarene bowl as cores with two triphenylene units as ancillary lateral columns (Figure 17(a)). The symmetrical calix[4]arene-linked triphenylene dimer **88** (Figure 18) with a C_{10} chain was such a case that exhibited the liquid-crystalline behaviour of a calixarene bowl as core with two triphenylene units as ancillary lateral columns [88]. Another way was triphenylene as cores, that is triphenylene column with calixarene units on ancillary lateral sides as shown in Figure 17(b). Compounds **89** and **90** were such cases that exhibited interesting mesomorphic behaviour of triphenylene column with calix[4]arene units on ancillary lateral sides [89].

Interestingly, Yang et al. synthesised symmetrical triads of triphenylene-calix[4]arene-triphenylenes **91** bridged by hydrazone spacers (Figure 19) [90]. It was found that these compounds showed interesting ion-

complexation-induced mesomorphic conversion between two distinct columnar phases. The neat compounds **91** showed mesophase with calixarene's bowl as cores. The Ag^+ complexes of **91** exhibited mesophase with triphenylene column as cores. Recently, another calixarene-linked discotic triphenylenes **92** were synthesised via click chemistry. The neat compounds **92** showed mesophase but their complexes with metallic salts exhibited no LC behaviours [91].

4. New advances of bowl LCs

4.1. Supramolecular bowl LCs

Another idea to stabilise such polar bowl structures is to use a hydrogen bonding (H-bonding). Many researchers have attempted to find the columnar LCs based on such structural concept [92–96]. Miyajima et al. reported that the fan-shaped molecules **93–95**

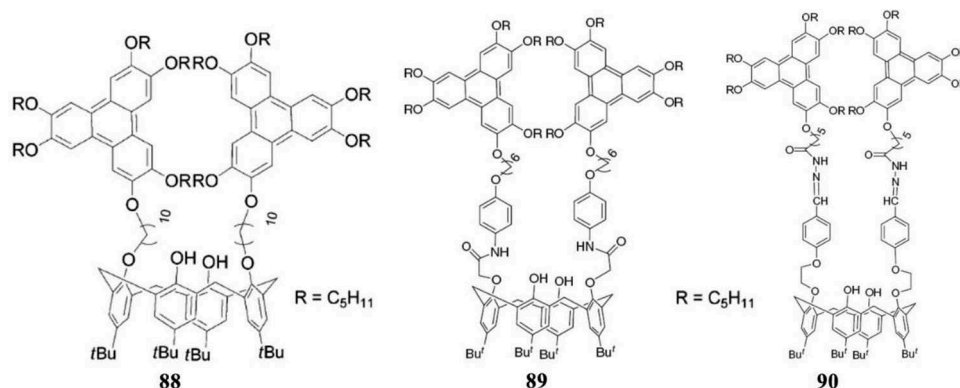


Figure 18. Chemical structures of triphenylene-calixarene-triphenylene **88–90**.

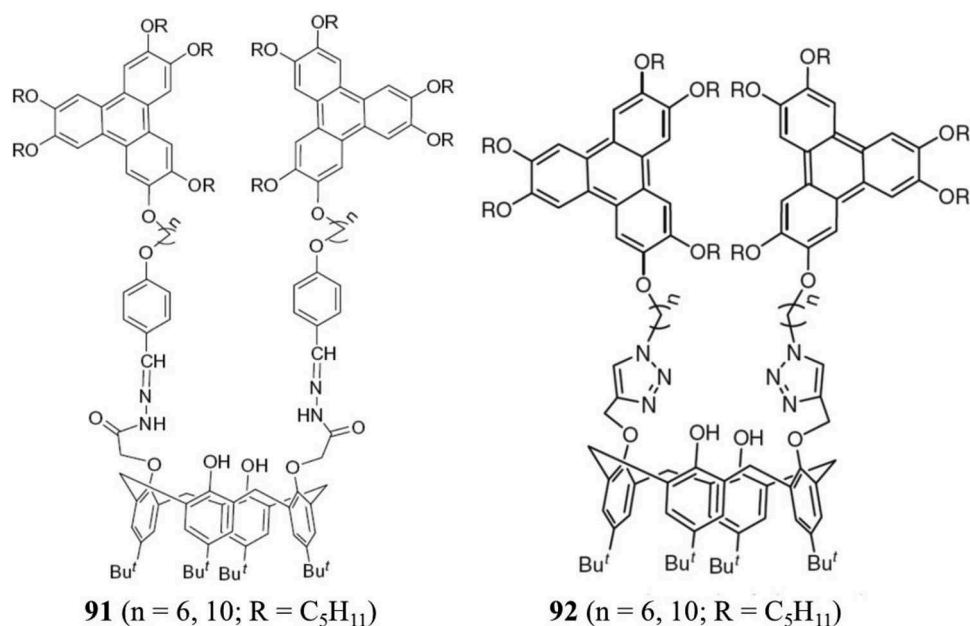


Figure 19. Chemical structures of triphenylene-calixarene-triphenylene **91** and **92**.

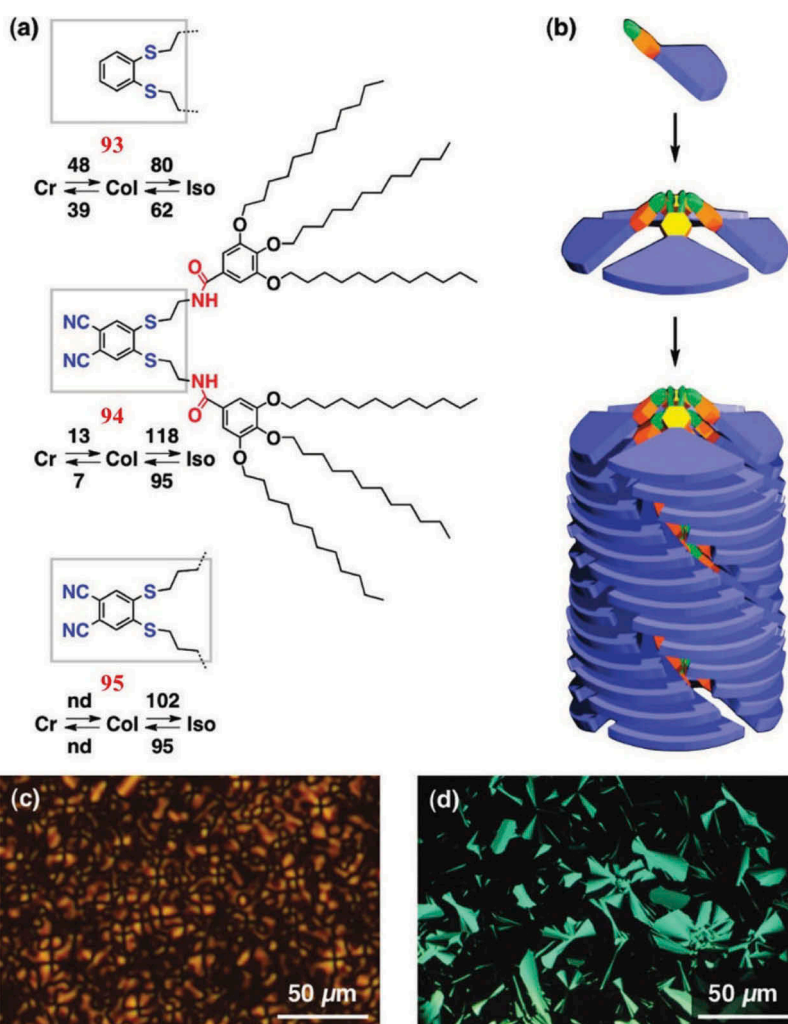


Figure 20. (a) Chemical structures of fan-shaped molecules **93**–**95** (phase transition temperatures in °C) and (b) illustration of their columnar assembly via hydrogen bonding. Optical textures of (c) **94** and (d) **95** at 90 and 80°C, respectively.

self-assembled conically into an umbrella, which stacks up to form a bowl-like columnar LC structure (Figure 20(a,b)) [97]. The introduction of a large dipole into the focal core of such fan-shaped molecules was expected to obtain spontaneous macroscopic polarisation in the resulting LC mesophase. 4,5-Dithiaphthalonitrile derivatives **94** and **95** were thus designed and synthesised, where two H-bonding amide groups ensure their umbrella-shaped assemblies that are essential for polarised columns. They confirmed that **94** and **95** both formed the hexagonal columnar mesophases (Figure 20(c,d)). The columnar mesophase in **94** was found to possess a spontaneous macroscopic polarisation, whereas spontaneous polarisation was absent in the mesophase of H-bonded **95**.

Unfortunately, these LCs were not switchable ferroelectrics because its polarisation did not respond to the external electric field.

Recently, a breakthrough has been made to stabilise the bowl-shaped assembly of phthalonitrile derivatives **96** into supramolecular columns by designing appropriate molecules with hydrogen bonds as shown in Figure 21(a) [49]. Under an applied electric field, both columns and core cyano groups could be unidirectionally aligned, thereby generating an extremely large macroscopic remnant polarisation (Figure 21(b)). The non-centrosymmetry was further characterised by SHG measurements, for which polarisation switching was clearly observed (Figure 21(c)). To the best of our knowledge, this system is the first demonstration of intrinsic

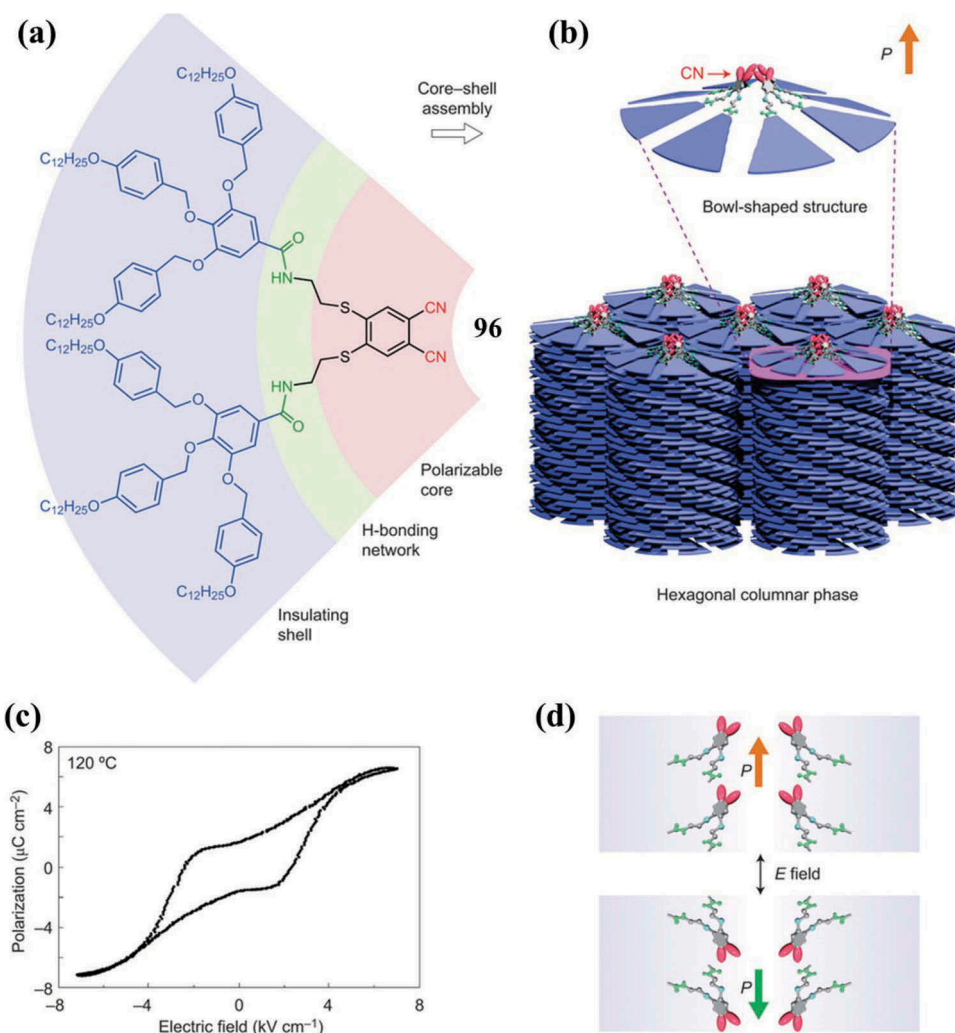


Figure 21. The chemical structure (a) of a mesogen **96** that assembles into a hexagonal columnar phase (b). Assembly proceeds by the segregation of four mesogens into a core-shell structure, with polar phthalonitrile units inside and the aliphatic side chains outside. (c) The intrinsic ferroelectric nature of the bowl-like columns is shown by the hysteresis of polarisation against electric field. (d) The cyano group in the core of the columns are either pointing up or down (according to the applied electric field) and yield a polar order parallel to the column axis (orange and green arrows for cyano groups pointing up and down, respectively). Reproduced with permission [100]. © 2015 Macmillan Publishers Limited.

ferroelectricity in a liquid-crystalline system without any treatment of the device surface or additional processing. The authors claimed that the phthalonitrile units instead of the hydrogen bonds were responsible for the ferroelectricity (Figure 21(d)). Although the polar amide units did not contribute to the ferroelectric effect, their bond polarisation ensured and maintained the unidirectional columnar orientation. The ferroelectric properties of this system were sensitive to several molecular parameters such as flexibility of the core, congestion of the shell structure, molecular packing within the core and intra-column hydrogen bonds. Interestingly, wet-processed LC films of such bowl-like columns with a high optical quality were also found to exhibit uniform spontaneous polarisation with a directional tunability under external electric field [98]. These features would lend superiority to the other conventional organic ferroelectrics in fabricating thin films, especially for device processing. Unlike the conventional ferroelectrics including the crystalline inorganic solids of barium titanate (BTO) and lead zirconate titanate (PZT), and polymer films of polyvinylidene fluoride, such supramolecular LCs could easily self-organise into large uniform ferroelectric domains in painted films or LC bulks, even nano-/micro-fibres and gels, which makes possible the easy fabrication of devices such as high-density memories, ferroelectric field-effect transistors and organic photovoltaic cells [99–104].

4.2. Liquid-crystalline corannulenes

Corannulene was first prepared in 1966 and characterised as a bowl-shaped polynuclear aromatic hydrocarbon. Corannulene is also known as a bucky-bowl due to its unique connection and bowl shape [105–110]. Aida et al. reported the first corannulene derivatives **98** and **99** that were able to form a liquid-crystalline assembly (Figure 22) [111]. In particular, compound **99** was found to form a hexagonal columnar LC assembly over a wide temperature range including room temperature. On cooling from the isotropic melt of **99**, the resulting fluidic LCs in polarised optical microscopy at 115°C clearly showed a fan texture (Figure 23(c)), which indicated the characteristic hexagonal columnar LC assemblies. XRD analysis of **99** at 70°C showed diffraction peaks with d-spacings of 35.0, 20.2 and 17.5 Å (Figure 23(d)), which could be indexed as the (1 0 0), (1 1 0) and (2 0 0) reflections of a hexagonal columnar mesophase. A broad halo centred at 4.3 Å is typical of paraffinic domains in the molten state. Compared with **99**, corannulene **98** bearing linear paraffinic side chains formed a LC mesophase only in a very narrow and much higher temperature range. The

resulting fluidic material showed a LC texture at 165°C (Figure 23(a)), which was distinctively different from that of **99**. XRD analysis of **98** at 165°C showed a periodic pattern composed of an intense peak with a d-spacing of 28.3 Å, indexed as the (0 0 1) reflection, followed by other peaks due to higher order reflections up to (0 0 7) (Figure 23(b)). From this characteristic XRD pattern, **98** most likely adopts a lamellar structure in the LC state. Interestingly, it was found that the LC columns of assembled **99** can be aligned homeotropically to an ITO electrode surface under an applied electric field (Figure 23(c), inset). Furthermore, the pattern developed electrically could be maintained for a long period of time at 125°C even after the electric field was switched off. Recently, liquid-crystalline behaviours were also observed in fivefold symmetric substituted corannulene derivatives [112]. These new LC materials, tailored with molecularly engineered corannulenes, are expected to open a new door for a variety of interesting applications.

4.3. Liquid-crystalline subphthalocyanines

Subphthalocyanine is a rare example of π -conjugated aromatic molecules with a rigid tetrahedral structure [113,114]. They are composed of three isoindole units condensed around a boron atom which also bears an axial ligand perpendicular to the macrocyclic core. Subphthalocyanines have recently attracted significant technological interest in the fields of organic semiconductors and optoelectronics [115,116]. Guilleme et al. reported the bowl-shaped mesogens based on the C_3 -symmetric boron subphthalocyanine **100** (Figure 24) [117]. This bowl-like compound was found to exhibit columnar phase with permanent polar order along the columnar axis. The polarisation orientation could be developed under electric field application only when cooling the sample from the isotropic phase. The degree of polar order was large enough for device applications, not sensitive to electric fields of opposite sense, and can be conserved for weeks in the mesophase after the electric field was switched off. This unique effect was ascribed to the rigidity of the axial dipolar subphthalocyanine stacks.

Recently, Guilleme et al. designed and synthesised another subphthalocyanine-based bowl-like molecule **101** with switchable columnar nematics (Figure 25) [118]. An amide group incorporated between the central core and each of the three peripheral molecular segments were found to enhance the cohesive forces between neighbouring molecules, due to strong intermolecular hydrogen-bonding interactions along the column. As a result, the material showed a hexagonal columnar mesophase Col_h in a very broad temperature range. However, the

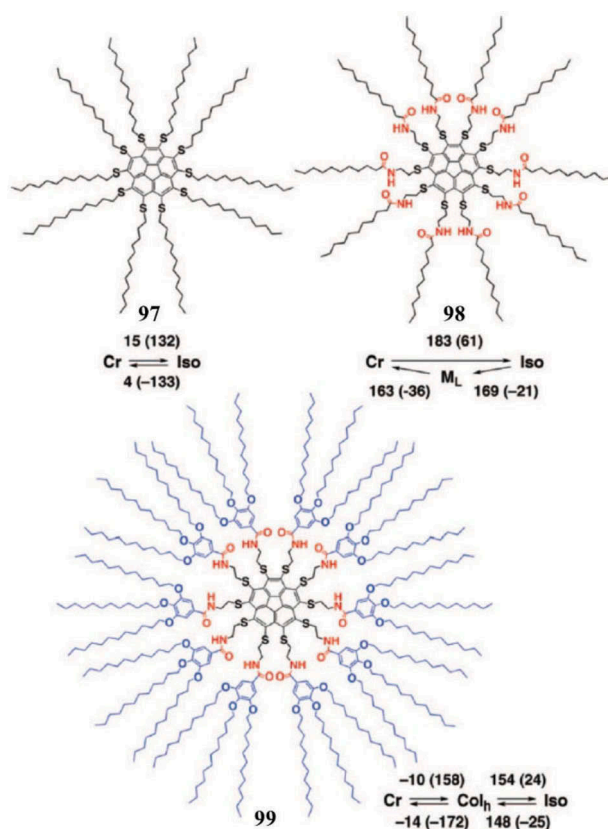


Figure 22. Chemical structures of corannulenes **97–99** and their liquid-crystalline properties. Cr, Col_h, M_L and I_{so} denote crystalline, hexagonal columnar, lamellar and isotropic phases, respectively.

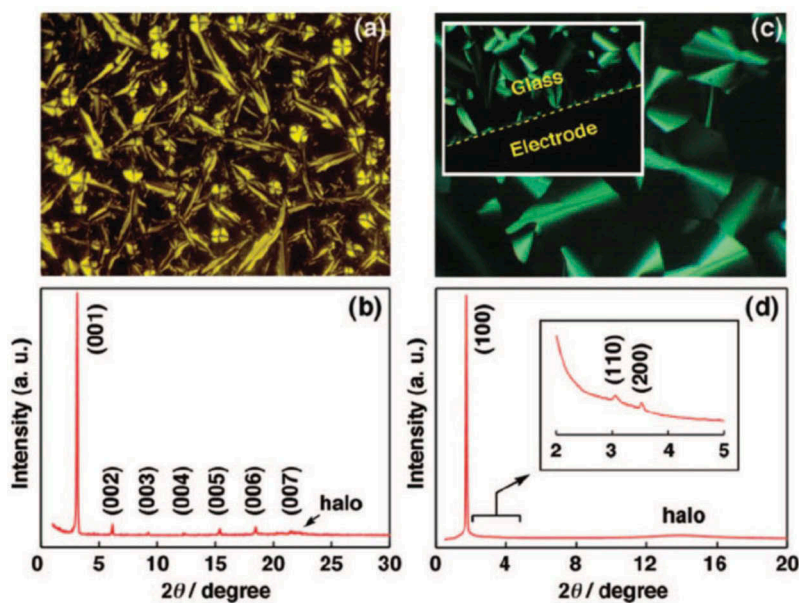


Figure 23. (a,c) Polarised optical micrographs of **98** at 165°C and **99** at 115°C. Inset in (c) shows optical texture at 125°C of **99**, sandwiched by glass plates with patterned ITO electrodes (5- μ m separation) under an applied electric field of 15 V/ μ m. (b,d) X-ray diffraction (XRD) patterns of **98** at 165°C and **99** at 70°C. Inset in (d) shows a magnified XRD pattern at $2\theta = 2^\circ\text{--}5^\circ$.

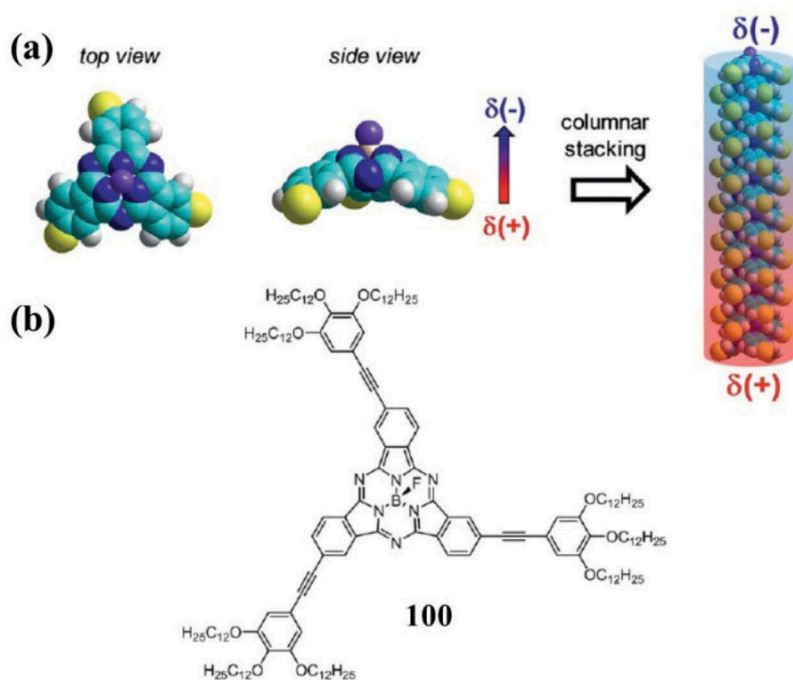


Figure 24. (a) Top and side views of the axial dipolar subphthalocyanine macrocycle. The yellow spheres represent the arylethynyl substituents. Head-to-tail stacking leads to polarised columnar structures. (b) Chemical structure of the C_3 -symmetric subphthalocyanine **100**.

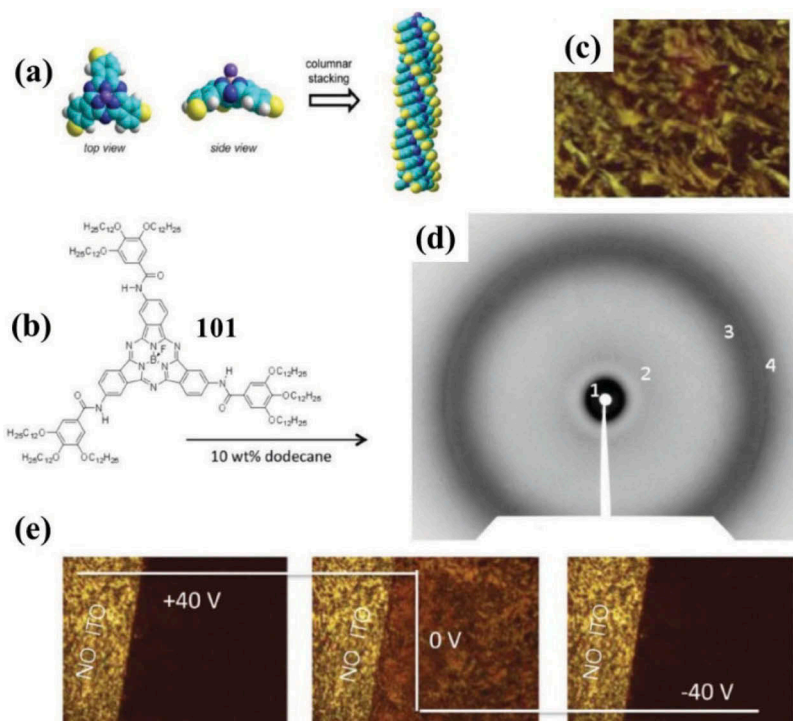


Figure 25. (a) Top and side views of the axial dipolar subphthalocyanine macrocycle and its packing in columns without the head-to-tail invariance. The yellow spheres represent the arylamide substituents. (b) Molecular structure of the bowlic subphthalocyanine **101**. (c) Optical texture of the lyotropic phase in dodecane (10 wt%). (d) X-ray diffraction pattern recorded at room temperature. (e) Textures observed by POM for the lyotropic mesophase in dodecane (10 wt%) under a low-frequency (0.1 Hz) square-wave field: left, +40 V; centre, transient texture observed during voltage inversion; right, -40 V. Sample thickness, 5 μm .

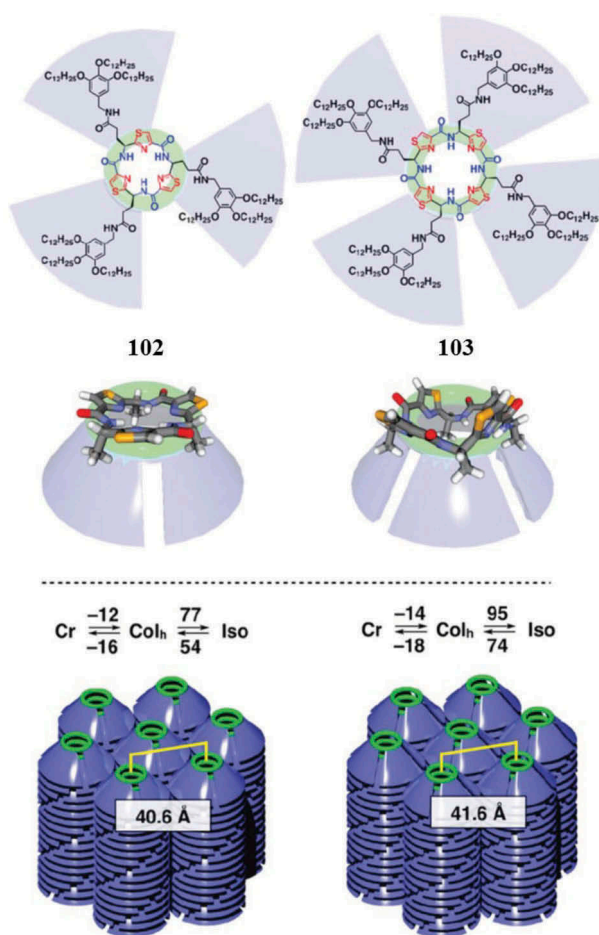


Figure 26. Molecular structures and phase transition diagrams of LC macrocyclic oligopeptide derivatives **102** and **103**. Their core units are bowl-shaped and self-organise columnarly with a hexagonal geometry.

high viscosity of the mesophase and the high temperatures of its range of stability are not ideal for processing and possible applications. Therefore, they tried to control these features by the addition of a suitable solvent. The low viscosity together with the kind of texture observed by polarised optical microscopy as shown in Figure 25(c) suggested the possibility of having a nematic phase at 10 wt%. XRD confirmed that this phase was a columnar nematic N_{Col} (Figure 25(d)). Interestingly, this lyotropic N_{Col} LCs exhibited polar response under the electric field (Figure 25(e)), which confirmed by texture observations and SHG methods. Since the LCs are lyotropic, uniform polar films could be easily fabricated simply by evaporating the solvent under an electric field. This could be of interest for the manufacture of thin-film electronic devices.

4.4. Liquid-crystalline peptidic macrocycles

Being inspired by naturally occurring peptidic macrocycles, Sato et al. developed liquid-crystalline compounds **102**

and **103** that were capable of self-organising into hexagonal columnar mesophases over a wide temperature range that includes room temperature (Figure 26) [119]. With the help of internal H-bonds, these macrocyclic peptides adopted a highly robust, bowl-shaped conformation with a large dipole moment. Differential scanning calorimetry analysis of **102** on second heating showed an LC mesophase over the temperature range from -12 to 77°C , which was characterised as hexagonal columnar (Col_h) phase by polarised optical microscopy and XRD analysis. Likewise, compound **103** was also found to self-assemble into hexagonal columnar (Col_h) phase from -14 to 95°C . Interestingly, they found that upon application of an electric field, the LC columns of both **102** and **103** underwent large-area unidirectional homeotropic orientation. It is also noteworthy that even after the electric field was switched off, the large-area unidirectional columnar orientation was maintained throughout an observation period of half a year. Amorín et al. demonstrated porous liquid-crystalline phases with an internal diameter of 7 \AA from self-assembling cyclic peptides decorated with mesogenic dendrons

[120]. The strategy took advantage of H-bonding interactions involving endocyclic amide groups and mesogenic driving forces promoted by polycatenar dendron-like benzoic acid derivatives. Moreover, Kawano et al. reported the columnar liquid-crystalline metallomacrocycles by the incorporation of the metal complexes inside the liquid-crystalline macrocycles [121].

4.5. Colloidal bowl-shaped nanoparticles

Various bowl-shaped nanoparticles and colloids have been recently designed, synthesised and characterised [122–127]. Their promising applications have been investigated in many aspects such as nanocontainer [124], superhydrophobic surfaces [125] and infrared-blocking coatings [126]. Marechal et al. explored the phase behaviour of bowl-shaped nanoparticles using confocal microscopy and computer simulations [50]. Experimentally, they observed the formation of a worm-like fluid phase, where the bowl-shaped particles were believed to stack on top of each other. Additionally, they performed Monte Carlo simulations, where the stacking and phase behaviour of hard bowl-shaped particles were investigated as a function of the thickness (or equivalently deepness). Figure 27 shows the phase diagram of hard bowl-shaped nanoparticles in the packing fraction (ϕ) versus thickness (D/σ) representation. Different stable crystal phases could be found. In the inverted crystal (IX) and the inverted braid-like crystal (IB), the particles were stacked in columns with half of the columns flipped upside down such that the rims of the bowls could interdigitate. In the IX, the resulting

columns were all aligned head to toe, while in the IB phase, the columns resemble braids with alternating tilt direction of the particles within each column. The solid hemispheres ($D = 0.5\sigma$) were found to exhibit two stable crystal structures, i.e. IX' and paired face-centred-cubic (fcc^2) phases. The IX' phase could be regarded as a sheared version of IX with alternating orientation of the particles and where the particles are not organised in columns. In the fcc^2 phase, the pairs of hemispheres joined together to form complete spheres that could rotate freely on the lattice positions of an fcc crystal. For $D/\sigma \leq 0.3$, an isotropic-to-columnar phase transition at intermediate densities was found. It was also found that columnar phase with all the particles pointing in the same direction was more stable than a columnar phase, where half of the columns were upside down. The work provides insight in the self-organisation of bowl-shaped nanoparticles, which is expected to provide guidance for designing molecular and nanometre-sized bowls as well as their liquid-crystalline properties and applications [128,129].

5. Conclusion and future prospects

In this review, we have outlined the history, advances and applications of bowl-like LCs. Bowl-like LCs were first proposed by the Chinese physicist Lui LAM in 1982. Since the discovery of bowl-like phases in CTV molecules by European scientists in 1985, a large amount of bowl-like liquid-crystalline materials have been developed based on various bowl-like cores including calixarenes, corannulenes, subphthalocyanines, peptidic macrocycles etc.

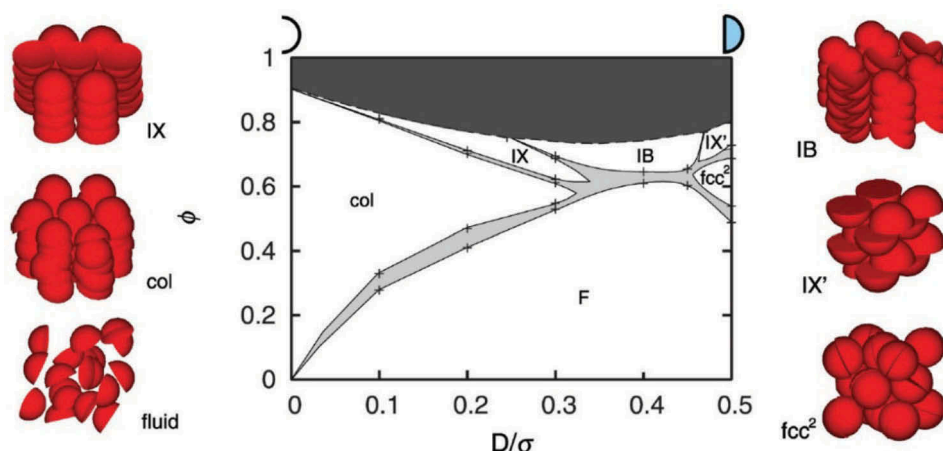


Figure 27. Phase diagram of hard bowl-shaped nanoparticles in the packing fraction (ϕ) versus thickness (D/σ). The light grey areas denote the coexistence regions, while the dark grey area indicates the forbidden region as it exceeds the maximum packing fraction of the bowls. The stable crystal phases, IX, IX', IB and fcc^2 [2], and the hexagonal columnar phase 'Col' are drawn schematically on the left and right of the figure. The lines are a guide to the eye. Reproduced with permission [50]. © 2010, American Chemical Society.

Different bowl-like mesophases such as columnar, nematic and smectic phases have been observed in bowl-shaped molecules by linking the bowl-like cores with multitudinous mesogenic groups and flexible side chains. The liquid-crystalline properties of colloidal bowl-shaped nanoparticles have also been explored. Interestingly, bowl-like ferroelectric columns have been achieved in the self-organised supramolecular systems with hydrogen bonding, and switchable ferroelectric columns have been observed in several bowl-like LCs. The genuine columnar ferroelectrics with the polarisation along the z axis (Ising type) in these bowl-like LCs could lead to new types of LCD with very fast response times and open a brand-new door for the development of ferroelectric or antiferroelectric soft materials with great potential applications in ultrahigh-density memory devices and beyond.

It is anticipated that bowl-like LCs could play an increasingly important role in the prosperous area of nanoscience and nanotechnology, and such a promising research field would also give rise to meaningful multidisciplinary cooperation of scientists and engineers from different backgrounds. However, since most of the related research endeavour in this burgeoning field remains in the preliminary stage, we may still have much chances to find new bowl-like LCs. Moreover, stimuli-responsive bowl-like LCs could be developed by incorporating the bowl-like cores with different responsive moieties, and chiral bowl-like LCs could be fabricated by introducing chiral centre in bowl-like molecules or doping chiral dopants into achiral bowl-like LCs as we do in rod-like and discotic systems [130–136]. For device applications, many problems and questions need to be further addressed. For example, the response speed of switchable ferroelectric columns in current systems is very slow. Much efforts should be devoted to the alignment control with suitable molecular orientations in the viscous columnar phases of bowl-like LCs by applying different external stimuli such as electric field, magnetic field, light and thermal treatment [137–139]. The relationships between molecular orientation and device performance should be investigated. Furthermore, bowl-like LC nanocomposites and their promising properties can be explored in the future. Bowl-like LCs could be used as templates to direct the self-assembly of colloidal particles or polymers. The dispersion of 1D and 2D nanostructures such as nanorods, nanotubes and graphene derivatives in bowl-like columnar nanostructures should enable the fabrication of even more complex 3D colloidal nanostructures for applications in micro/nanophotonics and other distinct areas, which would also be an ideal platform to control, explore and understand the organisation properties of different nanomaterials from the

nanometre to micrometre scales in a controllable and programmable technique [140–146]. Since the ground work done so far is encouraging, one can expect that the future breakthroughs in such promising topics would not only broaden our knowledge of soft matter but also promote their diverse applications as intelligent advanced functional materials.

Acknowledgements

The support from NASA: [Grant Number NASA-NNX13AQ60G] is gratefully acknowledged. We thank Prof. Ingo Dierking for kindly inviting us to write this review on bowl-like LCs for *Liquid Crystals Today*.

Disclosure statement

No potential conflict of interest was reported by the authors.

Funding

This work was supported by the NASA: [Grant Number NASA-NNX13AQ60G].

References

- [1] Priestly E. Introduction to liquid crystals. New York, NY: Springer Science & Business Media; 2012.
- [2] Collings PJ. Liquid crystals: nature's delicate phase of matter. Princeton, NJ: Princeton University Press; 2002.
- [3] Dierking I. Textures of liquid crystals. Weinheim: John Wiley & Sons; 2003.
- [4] Bisoyi HK, Li Q. Liquid crystals. Kirk-othmer encyclopedia of chemical technology. New York, NY: John Wiley & Sons; 2014.
- [5] Zheng ZG, Li Y, Bisoyi HK, et al. Three-dimensional control of the helical axis of a chiral nematic liquid crystal by light. *Nature*. 2016;531(7594):352–356.
- [6] Wang L, Li Q. Stimuli-responsive self-organized liquid crystalline nanostructures: from 1D to 3D photonic crystals. In: Comoretto D, editor. Organic and hybrid photonic crystals. Cham: Springer International Publishing; 2015. p. 393–430.
- [7] Bahr C, Kitzerow HS. Chirality in liquid crystals. Heidelberg: Springer; 2001.
- [8] Wang L, Li Q. Stimuli directing self-organized 3D liquid crystalline nanostructures: from materials design to photonic applications. *Adv Funct Mater*. 2016;26:10–28.
- [9] Zhao Y, Ikeda T. Smart light-responsive materials: azobenzene-containing polymers and liquid crystals. Hoboken, NJ: John Wiley & Sons; 2009.
- [10] Wang L. Self-activating liquid crystal devices for smart laser protection. *Liq Cryst*. 2016;43(13–15):2062–2078.
- [11] He WL, Wang L, Cui XP, et al. Wide temperature range blue phase liquid crystalline materials. *Prog Chem*. 2012;24:182–192.
- [12] Xie H, Wang L, Wang H, et al. Electrically tunable properties of wideband-absorptive and reflection-selective

- films based on multi-dichroic dye-doped cholesteric liquid crystals. *Liq Cryst.* **2015**;42(12):1698–1705.
- [13] Sun J, Wang H, Wang L, et al. Preparation and thermo-optical characteristics of a smart polymer-stabilized liquid crystal thin film based on smectic A-chiral nematic phase transition. *Smart Mater Struct.* **2014**;23(12):125038.
- [14] Gutierrez-Cuevas KG, Wang L, Zheng ZG, et al. Frequency-driven self-organized helical superstructures loaded with mesogen-grafted silica nanoparticles. *Angew Chem.* **2016**;128(42):13284–13288.
- [15] Zhang L, Wang M, Wang L, et al. Polymeric infrared reflective thin films with ultra-broad bandwidth. *Liq Cryst.* **2016**;43(6):750–757.
- [16] Lagerwall JP, Scalia G. A new era for liquid crystal research: applications of liquid crystals in soft matter nano-, bio- and microtechnology. *Cur Appl Phys.* **2012**;12(6):1387–1412.
- [17] Woltman SJ, Jay GD, Crawford GP. Liquid-crystal materials find a new order in biomedical applications. *Nat Mater.* **2007**;6(12):929–938.
- [18] Reinitzer F. Beiträge zur kenntniss des cholesterins. *Monatsh Chem.* **1888**;9(1):421–441.
- [19] Lehmann O. Über fließende krystalle. *Zeitschrift Für Physikalische Chemie.* **1889**;4(1):462–472.
- [20] Yeh P, Gu C. Optics of liquid crystal displays. Hoboken, NJ: John Wiley & Sons; **2010**.
- [21] Wu ST, Yang DK. Reflective liquid crystal displays. Hoboken, NJ: Wiley; **2001**.
- [22] Wang L, He W, Xiao X, et al. Hysteresis-free blue phase liquid-crystal-stabilized by ZnS nanoparticles. *Small.* **2012**;8(14):2189–2193.
- [23] Wang L, He W, Xiao X, et al. Low voltage and hysteresis-free blue phase liquid crystal dispersed by ferroelectric nanoparticles. *J Mater Chem.* **2012**;22(37):19629–19633.
- [24] Wang L, He W, Xiao X, et al. Wide blue phase range and electro-optical performances of liquid crystalline composites doped with thiophene-based mesogens. *J Mater Chem.* **2012**;22(6):2383–2386.
- [25] Kawamoto H. The history of liquid-crystal displays. *Proc IEEE.* **2002**;90(4):460–500.
- [26] Mara WC. Liquid crystal flat panel displays: manufacturing science & technology. New York, NY: Springer Science & Business Media; **2012**.
- [27] Chandrasekhar S. Liquid crystals of disk-like molecules. *Adv Liq Cryst.* **1982**;5:47–78.
- [28] Chandrasekhar S, Sadashiva BK, Suresh KA. Liquid crystals of disc-like molecules. *Pramana.* **1977**;9(5):471–480.
- [29] Isihara A. Theory of anisotropic colloidal solutions. *J Chem Phys.* **1951**;19(9):1142–1147.
- [30] Sergeev S, Pisula W, Geerts YH. Discotic liquid crystals: a new generation of organic semiconductors. *Chem Soc Rev.* **2007**;36(12):1902–1929.
- [31] Laschat S, Baro A, Steinke N, et al. Discotic liquid crystals: from tailor-made synthesis to plastic electronics. *Angew Chem Int Ed.* **2007**;46(26):4832–4887.
- [32] Kumar S. Self-organization of disc-like molecules: chemical aspects. *Chem Soc Rev.* **2006**;35(1):83–109.
- [33] Hird M. Ferroelectricity in liquid crystals-materials, properties and applications. *Liq Cryst.* **2011**;38(11–12):1467–1493.
- [34] Lagerwall ST. Ferroelectric and antiferroelectric liquid crystals. Weinheim: Wiley; **2008**.
- [35] Reddy RA, Tschierske C. Bent-core liquid crystals: polar order, superstructural chirality and spontaneous desymmetrisation in soft matter systems. *J Mater Chem.* **2006**;16(10):907–961.
- [36] Lin L. Wuli (Beijing). Liquid Crystals Phases and 'Dimensionality' of Molecules. **1982**;11:171.
- [37] Lin L. Bowlic liquid crystals. *Mol Cryst Liq Cryst.* **1987**;146(1):41–54. (Lam L.).
- [38] Lam L. The founding of the international liquid crystal society. All about science: philosophy, history, sociology & communication. Singapore: World Scientific; **2014**.
- [39] Leung KM, Lam L. Phase transitions of bowlic liquid crystals. *Mol Cryst Liq Cryst.* **1987**;146(1):71–76.
- [40] Lam L. Bowlics. In: Valery P, Shibaev, Lam L. editor. Liquid crystalline and mesomorphic polymers. New York: Springer; **1994**. p. 324–353.
- [41] Zimmermann H, Poupko R, Luz Z, et al. Pyramidic mesophases. *Zeitschrift Für Naturforschung A.* **1985**;40(2):149–160.
- [42] Malthete J, Collet A. Liquid crystals with a cone-shaped cyclotriveratrylene core. *Nouv J Chim.* **1985**;9(3):151–153.
- [43] Levelut AM, Malthete J, Collet A. X-ray structural study of the mesophases of some cone-shaped molecules. *J De Physique.* **1986**;47(2):351–357.
- [44] Lin L. Bowlic and polar liquid crystal polymers. *Mol Cryst Liq Cryst.* **1988**;155(1):531–538.
- [45] Zeng EM Design, synthesis and characterization of columnar discotic and bowlic liquid crystals. PhD thesis, Georgia Institute of Technology, Atlanta, **2001**.
- [46] Blinov LM. Structure and properties of liquid crystals. New York, NY: Springer Science & Business Media; **2010**.
- [47] Jakli A, Saupe A. Indication of ferroelectricity in columnar mesophases of pyramidic molecules. *Liq Cryst.* **1997**;22(3):309–316.
- [48] Xu B, Swager TM. Rigid bowlic liquid crystals based on tungsten-oxo calix [4] arenes: host-guest effects and head-to-tail organization. *J Am Chem Soc.* **1993**;115(3):1159–1160.
- [49] Miyajima D, Araoka F, Takezoe H, et al. Ferroelectric columnar liquid crystal featuring confined polar groups within core-shell architecture. *Science.* **2012**;336(6078):209–213.
- [50] Marechal M, Kortschot RJ, Demirörs AF, et al. Phase behavior and structure of a new colloidal model system of bowl-shaped particles. *Nano Lett.* **2010**;10(5):1907–1911.
- [51] Barón M, Stepto RF. Definitions of basic terms relating to polymer liquid crystals (IUPAC Recommendations 2001). *Pure Appl Chem.* **2002**;74(3):493–509.
- [52] Demus D, Goodby JW, Gray GW, et al., editors. Handbook of liquid crystals, low molecular weight liquid crystals I: calamitic liquid crystals. New York: Wiley; **2011**.
- [53] Robinson GM. A reaction of homopiperonyl and of homoveratryl alcohols. *J Chem Soc., Transactions.* **1915**;107:267–276.
- [54] Lindsey AS. 316. The structure of cyclotriveratrylene (10, 15-dihydro-2, 3, 7, 8, 12, 13-hexamethoxy-5 H-tribenzo [a, d, g] cyclononene) and related compounds. *J Chem Soc (Resumed).* **1965**:1685–1692.
- [55] Zimmermann H, Bader V, Poupko R, et al. Mesomorphism, isomerization, and dynamics in a new

- series of pyramidal liquid crystals. *J Am Chem Soc.* **2002**;124(51):15286–15301.
- [56] Collet A. Cyclotriveratrylenes and cryptophanes. *Tetrahedron.* **1987**;43(24):5725–5759.
- [57] Hardie MJ. Recent advances in the chemistry of cyclotriveratrylene. *Chem Soc Rev.* **2010**;39(2):516–527.
- [58] Zimmermann H, Poupko R, Luz Z, et al. Temperature dependent sign reversal of the optical anisotropy in pyramidal mesophases. *Zeitschrift Für Naturforschung A.* **1986**;41(9):1137–1140.
- [59] Dong Y, Chen D, Zeng E, et al. Disclination and molecular director studies on bowl-like columnar nematic phase using mosaic-like morphology decoration method. *Sci China Ser B: Chem.* **2009**;52(7):986–999.
- [60] Luz Z, Poupko R, Wachtel EJ, et al. Mesomorphic properties of the neat enantiomers of a chiral pyramidal liquid crystal. *Phys Chem Chem Phys.* **2009**;11(41):9562–9568.
- [61] Budig H, Lunkwitz R, Paschke R, et al. The influence of heteroatoms and branchings on the liquid-crystalline properties of cyclotriveratrylene derivatives. *J Mater Chem.* **1996**;6(8):1283–1289.
- [62] Lunkwitz R, Tschierske C, Diele S. Formation of smectic and columnar liquid crystalline phases by cyclotriveratrylene (CTV) and cyclotetraeratrylene (CTTV) derivatives incorporating calamitic structural units. *J Mater Chem.* **1997**;7(10):2001–2011.
- [63] Budig H, Diele S, Göring P, et al. Synthesis and investigations of new liquid-crystalline compounds by combination of the pyramidal tribenzocyclononene unit and calamitic structural units. *J Chem Soc., Perkin Transactions 2.* **1995**;4:767–775.
- [64] Budig H, Diele S, Göring P, et al. New liquid crystalline materials by combination of pyramidal and calamitic structural units. *J Chem Soc, Chem Commun.* **1994**;20:2359–2360.
- [65] Percec V, Cho CG, Pugh C, et al. Synthesis and characterization of branched liquid-crystalline polyethers containing cyclotetraeratrylene-based disk-like mesogens. *Macromolecules.* **1992**;25(3):1164–1176.
- [66] Zimmermann H, Poupko R, Luz Z, et al. Tetrabenzocyclododecatetraene A new core for mesogens exhibiting columnar mesophases. *Liq Cryst.* **1988**;3(6–7):759–770.
- [67] Malthete J, Collet A. Inversion of the cyclotribenzylene cone in a columnar mesophase: a potential way to ferroelectric materials. *J Am Chem Soc.* **1987**;109(24):7544–7545.
- [68] Peterca M, Percec V, Imam MR, et al. Molecular structure of helical supramolecular dendrimers. *J Am Chem Soc.* **2008**;130(44):14840–14852.
- [69] Percec V, Imam MR, Peterca M, et al. Self-assembly of dendritic crowns into chiral supramolecular spheres. *J Am Chem Soc.* **2009**;131(3):1294–1304.
- [70] Gutsche CD. *Calixarenes: an introduction.* Cambridge: Royal Society of Chemistry; **2008**.
- [71] Mz A, Böhmer V, Harrowfield J, et al., editors. *Calixarenes 2001.* New York, NY: Springer Science & Business Media; **2007**.
- [72] C.D. Gutsche, Calixarenes, In: Stoddart JF, editor. *Monographs in Supramolecular Chemistry,* Cambridge: Royal Society of Chemistry; **1989**. p. 1.
- [73] Schurig V. The reciprocal principle of selectand-selector-systems in supramolecular chromatography. *Molecules.* **2016**;21(11):1535.
- [74] Joseph R, Rao CP. Ion and molecular recognition by lower rim 1, 3-di-conjugates of calix [4] arene as receptors. *Chem Rev.* **2011**;111(8):4658–4702.
- [75] Yang F, Guo H, Vicens J. Mini-review: calixarene liquid crystals. *J Incl Phenom Macrocycl Chem.* **2014**;80(3–4):177–186.
- [76] Swager TM, Xu B. Liquid crystalline calixarenes. *J Incl Phenom Macrocycl Chem.* **1994**;19(1):389–398.
- [77] Cometti G, Dalcanale E, Du Vosel A, et al. New bowl-shaped columnar liquid crystals. *J Chem Soc, Chem Commun.* **1990**(2): 163–165.
- [78] Budig H, Diele S, Paschke R, et al. Mesomorphic properties and monolayer behaviour of novel liquid crystalline exo-calix [4] arene derivatives. *J Chem Soc., Perkin Transactions 2.* **1996**;9:1901–1906.
- [79] Yonetake K, Nakayama T, Ueda M. New liquid crystals based on calixarenes. *J Mater Chem.* **2001**;11(3):761–767.
- [80] Lo PK, Chen D, Meng Q, et al. Highly ordered smectic phases from polar calix [4] arene derivatives. *Chem Mater.* **2006**;18(17):3924–3930.
- [81] Menon SK, Patel RK, Panchal JG, et al. Dielectric study of novel liquid crystals based on calix [4] arene Schiff bases. *Liq Cryst.* **2011**;38(2):123–134.
- [82] Patel RV, Panchal JG, Rana VA, et al. Liquid crystals based on calix [4] arene Schiff bases. *J Incl Phenom Macrocycl Chem.* **2010**;66(3–4):285–295.
- [83] Romero J, Barberá J, Blesa MJ, et al. Liquid crystal organization of calix[4]arene-appended Schiff bases and recognition towards Zn²⁺. *ChemistrySelect.* **2017**;2(1):101–109.
- [84] Zhang X, Guo H, Yang F, et al. Ion complexation-controlled columnar mesophase of calix [4] arene-cholesterol derivatives with Schiff-base bridges. *Tetrahedron Lett.* **2016**;57(8):905–909.
- [85] Xu B, Swager TM. Host-guest mesomorphism: cooperative stabilization of a bowl-like columnar phase. *J Am Chem Soc.* **1995**;117(17):5011–5012.
- [86] Sutariya PG, Modi NR, Pandya A, et al. Synthesis, mesomorphism and dielectric behaviour of novel basket shaped scaffolds constructed on lower rim azocalix [4] arenes. *RSC Adv.* **2013**;3(13):4176–4180.
- [87] Fang X, Guo H, Yang F, et al. Novel gallic-calixarene liquid crystals: syntheses and conformation influences on mesomorphism. *Tetrahedron Lett.* **2015**;56(44):6128–6131.
- [88] Yang F, Guo H, Xie J, et al. Synthesis of calixarene-linked discotic triphenylene. *Eur J Org Chem.* **2011**;2011(26):5141–5145.
- [89] Yang F, Xu B, Guo H, et al. Novel symmetrical triads of triphenylene-calix [4] arene-triphenylene: synthesis and mesomorphism. *Tetrahedron Lett.* **2012**;53(13):1598–1602.

- [90] Yang F, Bai X, Guo H, et al. Ion complexation-induced mesomorphic conversion between two columnar phases of novel symmetrical triads of triphenylene-calix [4] arene-triphenylenes. *Tetrahedron Lett.* **2013**;54(5):409–413.
- [91] Hong B, Yang F, Guo H, et al. Synthesis, complexation, and mesomorphism of novel calixarene-linked discotic triphenylene based on click chemistry. *Tetrahedron Lett.* **2014**;55(1):252–255.
- [92] Barbera J, Iglesias R, Serrano JL, et al. Switchable columnar metallomesogens. *New Helical Self-Assembling Systems.* *J. Am. Chem. Soc.* **1998**;120(12):2908–2918.
- [93] Goodby JW, Mehl GH, Saez IM, et al. Liquid crystals with restricted molecular topologies: supermolecules and supramolecular assemblies. *Chem Commun.* **1998**;19:2057–2070.
- [94] Velayutham TS, Ng BK, Gan WC, et al. Phase sensitive molecular dynamics of self-assembly glycolipid thin films: a dielectric spectroscopy investigation. *J Chem Phys.* **2014**;141(8):08B617–1.
- [95] Velayutham TS, Nguan HS, Ng BK, et al. Molecular dynamics of anhydrous glycolipid self-assembly in lamellar and hexagonal phases. *Phys Chem Chem Phys.* **2016**;18(22):15182–15190.
- [96] Serrette AG, Swager TM. Polar superstructures stabilized by polymeric xxometal units: columnar liquid crystals based on tapered dioxomolybdenum complexes. *Angew Chem Int Ed.* **1994**;33(22):2342–2345.
- [97] Miyajima D, Araoka F, Takezoe H, et al. Columnar liquid crystal with a spontaneous polarization along the columnar axis. *J Am Chem Soc.* **2010**;132(25):8530–8531.
- [98] Araoka F, Masuko S, Kogure A, et al. High-optical-quality ferroelectric film wet-processed from a ferroelectric columnar liquid crystal as observed by non-linear-optical microscopy. *Adv Mater.* **2013**;25(29):4014–4017.
- [99] Takezoe H, Kishikawa K, Gorecka E. Switchable columnar phases. *J Mater Chem.* **2006**;16(25):2412–2416.
- [100] Tayi AS, Kaeser A, Matsumoto M, et al. Supramolecular ferroelectrics. *Nature Chem.* **2015**;7(4):281–294.
- [101] Takezoe H, Araoka F. Polar columnar liquid crystals. *Liq Cryst.* **2014**;41(3):393–401.
- [102] Takezoe H. Historical overview of polar liquid crystals. *Ferroelectrics.* **2014**;468(1):1–7.
- [103] Araoka F, Isoda M, Miyajima D, et al. Polar dynamics at a functional group level: infrared-visible sum-frequency generation study on polar columnar liquid crystals. *Adv Electron Mater.* **2017**;3(3):1600503.
- [104] Araoka F, Takezoe H. Columnar liquid crystal as a unique ferroelectric liquid crystal. *Jap J Appl Phys.* **2013**;53(15):01AA01.
- [105] Barth WE, Lawton RG. Dibenzo [ghi, mno] fluoranthene. *J Am Chem Soc.* **1966**;88(2):380–381.
- [106] Kawase T, Kurata H. Ball-, bowl-, and belt-shaped conjugated systems and their complexing abilities: exploration of the concave-convex π - π interaction. *Chem Rev.* **2006**;106(12):5250–5273.
- [107] Lawton RG, Barth WE. Synthesis of corannulene. *J Am Chem Soc.* **1971**;93(7):1730–1745.
- [108] Seiders TJ, Elliott EL, Grube GH, et al. Synthesis of corannulene and alkyl derivatives of corannulene. *J Am Chem Soc.* **1999**;121(34):7804–7813.
- [109] Butterfield AM, Gilomen B, Siegel JS. Kilogram-scale production of corannulene. *Org Process Res Dev.* **2012**;16(4):664–676.
- [110] Wu YT, Siegel JS. Aromatic molecular-bowl hydrocarbons: synthetic derivatives, their structures, and physical properties. *Chem Rev.* **2006**;106(12):4843–4867.
- [111] Miyajima D, Tashiro K, Araoka F, et al. Liquid crystalline corannulene responsive to electric field. *J Am Chem Soc.* **2008**;131(1):44–45.
- [112] Mattarella M, Haberl JM, Ruokolainen J, et al. Five-fold symmetric penta-substituted corannulene with gelation properties and a liquid-crystalline phase. *Chem Commun.* **2013**;49(65):7204–7206.
- [113] Claessens CG, González-Rodríguez D, Torres T. Subphthalocyanines: singular nonplanar aromatic compounds synthesis, reactivity, and physical properties. *Chem Rev.* **2002**;102(3):835–854.
- [114] Claessens CG, González-Rodríguez D, Rodríguez-Morgade MS, et al. Subphthalocyanines, subporphyrines, and subporphyrins: singular nonplanar aromatic systems. *Chem Rev.* **2013**;114(4):2192–2277.
- [115] Guilleme J, Mayoral MJ, Calbo J, et al. Non centrosymmetric homochiral supramolecular polymers of tetrahedral subphthalocyanine molecules. *Angew Chem Int Ed.* **2015**;54(8):2543–2547.
- [116] Menke SM, Luhman WA, Holmes RJ. Tailored exciton diffusion in organic photovoltaic cells for enhanced power conversion efficiency. *Nature Mater.* **2013**;12(2):152.
- [117] Guilleme J, Aragó J, Ortí E, et al. A columnar liquid crystal with permanent polar order. *J Mater Chem C.* **2015**;3(5):985–989.
- [118] Guilleme J, Cavero E, Sierra T, et al. Polar switching in a lyotropic columnar nematic liquid crystal made of bowl-shaped molecules. *Adv Mater.* **2015**;27(29):4280–4284.
- [119] Sato K, Itoh Y, Aida T. Columnar assembled liquid-crystalline peptidic macrocycles unidirectionally orientable over a large area by an electric field. *J Am Chem Soc.* **2011**;133(35):13767–13769.
- [120] Amorín M, Pérez A, Barberá J, et al. Liquid crystal organization of self-assembling cyclic peptides. *Chem Commun.* **2014**;50(6):688–690.
- [121] Kawano SI, Ishida Y, Tanaka K. Columnar liquid-crystalline metallomacrocycles. *J Am Chem Soc.* **2015**;137(6):2295–2302.
- [122] Wang XD, Graugnard E, King JS, et al. Large-scale fabrication of ordered nanobowl arrays. *Nano Lett.* **2004**;4(11):2223–2226.
- [123] Charnay C, Lee A, Man SQ, et al. Reduced symmetry metallodielectric nanoparticles: chemical synthesis and plasmonic properties. *J Phys Chem B.* **2003**;107(30):7327–7333.
- [124] Jagadeesan D, Mansoori U, Mandal P, et al. Hollow spheres to nanocups: tuning the morphology and magnetic properties of single-crystalline α -Fe₂O₃ nanostructures. *Angew Chem Int Ed.* **2008**;47(40):7685–7688.
- [125] Love JC, Gates BD, Wolfe DB, et al. Fabrication and wetting properties of metallic half-shells with submicron diameters. *Nano Lett.* **2002**;2(8):891–894.
- [126] Liu J, Maarooft AI, Wiecek L, et al. Fabrication of hollow metal “nanocaps” and their red-shifted optical absorption spectra. *Adv Mater.* **2005**;17(10):1276–1281.

- [127] Hosein ID, Liddell CM. Convectively assembled non-spherical mushroom cap-based colloidal crystals. *Langmuir*. 2007;23(17):8810–8814.
- [128] Marechal M, Dijkstra M. Phase behavior and structure of colloidal bowl-shaped particles: simulations. *Phys Rev E*. 2010;82(3):031405.
- [129] De Graaf J, Van Roij R, Dijkstra M. Dense regular packings of irregular nonconvex particles. *Phys Rev Lett*. 2011;107(15):155501.
- [130] Li Q. Intelligent stimuli-responsive materials: from well-defined nanostructures to applications. New York: Wiley; 2013.
- [131] Wang L, Dong H, Li Y, et al. Reversible near-infrared light directed reflection in a self-organized helical superstructure loaded with upconversion nanoparticles. *J Am Chem Soc*. 2014;136(12):4480–4483.
- [132] Wang L, Dong H, Li Y, et al. Luminescence-driven reversible handedness inversion of self-organized helical superstructures enabled by a novel near-infrared light nanotransducer. *Adv Mater*. 2015;27(12):2065–2069.
- [133] Chen X, Wang L, Li C, et al. Light-controllable reflection wavelength of blue phase liquid crystals doped with azobenzene-dimers. *Chem Commun*. 2013;49(86):10097–10099.
- [134] Lee YH, Wang L, Yang H, et al. Photo-induced handedness inversion with opposite-handed cholesteric liquid crystal. *Optics Express*. 2015;23(17):22658–22666.
- [135] Chen G, Wang L, Wang Q, et al. Photoinduced hyper-reflective laminated liquid crystal film with simultaneous multicolor reflection. *ACS Appl Mater Int*. 2014;6(3):1380–1384.
- [136] Wang L, Gutierrez-Cuevas KG, Bisoyi HK, et al. NIR light-directing self-organized 3D photonic superstructures loaded with anisotropic plasmonic hybrid nanorods. *Chem Commun*. 2015;51(81):15039–15042.
- [137] Takatoh K, Sakamoto M, Hasegawa R, et al. Alignment technology and applications of liquid crystal devices. New York, NY: CRC Press; 2005.
- [138] Xue C, Xiang J, Nemati H, et al. Light-driven reversible alignment switching of liquid crystals enabled by azo thiol grafted gold nanoparticles. *Chem Phys Chem*. 2015;16(9):1852–1856.
- [139] Ichimura K. Photoalignment of liquid-crystal systems. *Chem Rev*. 2000;100(5):1847–1874.
- [140] Mitov M, Portet C, Bourgerette C, et al. Long-range structuring of nanoparticles by mimicry of a cholesteric liquid crystal. *Nature Mater*. 2002;1(4):229–231.
- [141] Vallooran JJ, Bolisetty S, Mezzenga R. Macroscopic alignment of lyotropic liquid crystals using magnetic nanoparticles. *Adv Mater*. 2011;23(34):3932–3937.
- [142] Bisoyi HK, Kumar S. Liquid-crystal nanoscience: an emerging avenue of soft self-assembly. *Chem Soc Rev*. 2011;40(1):306–319.
- [143] Gutierrez-Cuevas KG, Wang L, Xue C, et al. Near infrared light-driven liquid crystal phase transition enabled by hydrophobic mesogen grafted plasmonic gold nanorods. *Chem Commun*. 2015;51(48):9845–9848.
- [144] Wang L, Gutierrez-Cuevas KG, Urbas A, et al. Near-infrared light-directed handedness inversion in plasmonic nanorod-embedded helical superstructure. *Adv Opt Mater*. 2016;4(2):247–251.
- [145] Lynch MD, Patrick DL. Organizing carbon nanotubes with liquid crystals. *Nano Lett*. 2002;2(11):1197–1201.
- [146] Serra F, Yang S. Liquid crystals: material defect lines. *Nature Mater*. 2016;15(1):10–11.